

Investigation of the Mechanism of C(sp³)–H Bond Cleavage in Pd(0)-Catalyzed Intramolecular Alkane Arylation Adjacent to Amides and Sulfonamides

Sophie Rousseaux,* Serge I. Gorelsky, Benjamin K. W. Chung, and Keith Fagnou

Centre for Catalysis Research and Innovation, Department of Chemistry, University of Ottawa, 10 Marie Curie, Ottawa, Ontario, K1N 6N5, Canada

Received April 12, 2010; E-mail: srous100@uottawa.ca

Abstract: The reactivity of C(sp³)–H bonds adjacent to a nitrogen atom can be tuned to allow intramolecular alkane arylation under Pd(0) catalysis. Diminishing the Lewis basicity of the nitrogen lone pair is crucial for this catalytic activity. A range of *N*-methanamides and sulfonamides react exclusively at primary C(sp³)–H bonds to afford the products of alkane arylation in good yields. The isolation of a Pd(II) reaction intermediate has enabled an evaluation of the reaction mechanism with a focus on the role of the bases in the C(sp³)–H bond cleaving step. The results of these stoichiometric studies, together with kinetic isotope effect experiments, provide rare experimental support for a concerted metalation–deprotonation (CMD) transition state, which has previously been proposed in alkane C(sp³)–H arylation. Moreover, DFT calculations have uncovered the additional role of the pivalate additive as a promoter of phosphine dissociation from the Pd(II) intermediate, enabling the CMD transition state. Finally, kinetic studies were performed, revealing the reaction rate expression and its relationship with the concentration of pivalate.

1. Introduction

In recent years, significant progress has been made in the establishment of transition-metal catalyzed transformations at sp³ carbon–hydrogen bonds for the formation of carbon–carbon,^{1–4} carbon–halide,⁵ carbon–boron,⁶ carbon–silicon,⁷ carbon–oxygen,⁸ carbon–nitrogen,⁹ and carbon–sulfur¹⁰ bonds.^{11,12} Within the domain of carbon–carbon bond formation, mechanistic investigations related to catalytic transformations at arene, heteroarene, and alkene C(sp²)–H bonds have enabled chemists to extend the boundaries of substrates that may be functionalized to include a wide scope of synthetically useful motifs.^{13–16} However, the development of catalytic C–C bond formations at nonacidic C(sp³)–H bonds has been less forthcoming,^{11,12,17,18}

since these systems do not benefit from catalyst–reactant interactions through the π -system of the substrate, as opposed to their sp² hybridized counterparts.¹⁹

In the context of transition-metal catalyzed arylations at C(sp²)–H bonds, the mechanism of C–H bond cleavage is currently the subject of much discussion. Several groups have

- (1) For examples of Pd(II)/Pd(0)-catalyzed transformations at C(sp³)–H bonds for C–C bond formation: (a) Periana, R. A.; Mironov, O.; Taube, D.; Bhalla, G.; Jones, C. J. *Science* **2003**, *301*, 814. (b) Zerella, M.; Mukhopadhyay, S.; Bell, A. T. *Chem. Commun.* **2004**, 1948. (c) Chen, X.; Goodhue, C. E.; Yu, J.-Q. *J. Am. Chem. Soc.* **2006**, *128*, 12634. (d) Giri, R.; Maugel, N.; Li, J.-J.; Wang, D.-H.; Breazzano, S. P.; Saunders, L. B.; Yu, J.-Q. *J. Am. Chem. Soc.* **2007**, *129*, 3510. (e) Wang, D.-H.; Wasa, M.; Giri, R.; Yu, J.-Q. *J. Am. Chem. Soc.* **2008**, *130*, 7190. (f) Shi, B.-F.; Maugel, N.; Zhang, Y.-H.; Yu, J.-Q. *Angew. Chem., Int. Ed.* **2008**, *47*, 4882. (g) Lin, S.; Song, C.-X.; Cai, G.-X.; Wang, W.-H.; Shi, Z.-J. *J. Am. Chem. Soc.* **2008**, *130*, 12901. (h) Young, A. J.; White, M. C. *J. Am. Chem. Soc.* **2008**, *130*, 14090. (i) Liégault, B.; Fagnou, K. *Organometallics* **2008**, *27*, 4841. (j) Wasa, M.; Engle, K. M.; Yu, J.-Q. *J. Am. Chem. Soc.* **2010**, *132*, 3680.
- (2) For examples of Pd(II)/Pd(IV)-catalyzed transformations at C(sp³)–H bonds for C–C bond formation: (a) Catellani, M.; Motti, E.; Ghelli, S. *Chem. Commun.* **2000**, 2003. (b) Zaitsev, V. D.; Shabashov, D.; Daugulis, O. *J. Am. Chem. Soc.* **2005**, *127*, 13154. (c) Kalyani, D.; Deprez, N. R.; Desai, L. V.; Sanford, M. S. *J. Am. Chem. Soc.* **2005**, *127*, 7330. (d) Shabashov, D.; Daugulis, O. *Org. Lett.* **2005**, *7*, 3657. (e) Reddy, B. V. S.; Reddy, L. R.; Corey, E. J. *Org. Lett.* **2006**, *8*, 3391. (f) Deprez, N. R.; Sanford, M. S. *J. Am. Chem. Soc.* **2009**, *131*, 11234. (g) Shabashov, D.; Daugulis, O. *J. Am. Chem. Soc.* **2010**, *132*, 3965. See also ref 1d.

- (3) For examples of Pd(0)/Pd(II)-catalyzed transformations at C(sp³)–H bonds for C–C bond formation: (a) Dyker, G. *Angew. Chem., Int. Ed. Engl.* **1992**, *31*, 1023. (b) Dyker, G. *J. Org. Chem.* **1993**, *58*, 6426. (c) Dyker, G. *Angew. Chem., Int. Ed. Engl.* **1994**, *33*, 103. (d) Baudoin, O.; Herrbach, A.; Guéritte, F. *Angew. Chem., Int. Ed.* **2003**, *42*, 5736. (e) Zhao, J.; Campo, M.; Larock, R. C. *Angew. Chem., Int. Ed.* **2005**, *44*, 1873. (f) Barder, T. E.; Walker, S. D.; Martinelli, J. R.; Buchwald, S. L. *J. Am. Chem. Soc.* **2005**, *127*, 4685. (g) Ren, H.; Knochel, P. *Angew. Chem., Int. Ed.* **2006**, *45*, 3462. (h) Dong, C.-G.; Hu, Q.-S. *Angew. Chem., Int. Ed.* **2006**, *45*, 2289. (i) Dong, C.-G.; Hu, Q.-S. *Org. Lett.* **2006**, *8*, 5057. (j) Lafrance, M.; Gorelsky, S. I.; Fagnou, K. *J. Am. Chem. Soc.* **2007**, *129*, 14570. (k) Niwa, T.; Yorimitsu, H.; Oshima, K. *Org. Lett.* **2007**, *9*, 2373. (l) Ren, H.; Li, Z.; Knochel, P. *Chem. Asian J.* **2007**, *2*, 416. (m) Hitce, J.; Retaillieu, P.; Baudoin, O. *Chem.–Eur. J.* **2007**, *13*, 792. (n) Dong, C.-G.; Yeung, P.; Hu, Q.-S. *Org. Lett.* **2007**, *9*, 363. (o) Liron, F.; Knochel, P. *Tetrahedron Lett.* **2007**, *48*, 4943. (p) Campeau, L.-C.; Schipper, D. J.; Fagnou, K. *J. Am. Chem. Soc.* **2008**, *130*, 3266. (q) Mousseau, J. J.; Larivée, A.; Charette, A. B. *Org. Lett.* **2008**, *10*, 1641. (r) Niwa, T.; Yorimitsu, H.; Oshima, K. *Org. Lett.* **2008**, *10*, 4689. (s) Watanabe, T.; Oishi, S.; Fujii, N.; Ohno, H. *Org. Lett.* **2008**, *10*, 1759. (t) Kim, H. S.; Gowrisankar, S.; Kim, S. H.; Kim, J. N. *Tetrahedron Lett.* **2008**, *49*, 3858. (u) Dong, C.-G.; Hu, Q.-S. *Tetrahedron* **2008**, *64*, 2537. (v) Chaumontet, M.; Piccardi, R.; Audic, N.; Hitce, J.; Peglion, J.-L.; Clot, E.; Baudoin, O. *J. Am. Chem. Soc.* **2008**, *130*, 15157. (w) Salcedo, A.; Neuville, L.; Zhu, J. *J. Org. Chem.* **2008**, *73*, 3600. (x) Schipper, D. J.; Campeau, L.-C.; Fagnou, K. *Tetrahedron* **2009**, *65*, 3155. (y) Wasa, M.; Engle, K. M.; Yu, J.-Q. *J. Am. Chem. Soc.* **2009**, *131*, 9886. (z) Chaumontet, M.; Piccardi, R.; Baudoin, O. *Angew. Chem., Int. Ed.* **2009**, *48*, 179. (aa) Chaumontet, M.; Retaillieu, P.; Baudoin, O. *J. Org. Chem.* **2009**, *74*, 1774. (ab) Liu, T.-P.; Xing, C.-H.; Hu, Q.-S. *Angew. Chem., Int. Ed.* **2010**, *49*, 2909.

validated a concerted metalation–deprotonation (CMD) pathway for C–C bond formation at C(sp²)-H bonds with computational and experimental studies.^{20,21} This mechanism features C(sp²)-H deprotonation with concomitant (hetero)arene metalation. Importantly, the concerted nature of this process opens the door for similar reactivity at nonacidic C(sp³)-H bonds which cannot react in a stepwise fashion.

Due to the tolerance of a wide range of functional groups in Pd(0) catalysis, our group^{3j,p,x} and others have investigated its use in C–C bond formation at C(sp³)-H bonds.³ The preference for Pd(0) catalysis lies in the ability to use inexpensive, commercially available (or easily accessible) aryl bromides and chlorides as coupling partners. While the aryl halide remains an element of preactivation in the coupling process, it also enables the necessary change in metal oxidation state for C–H bond cleavage to occur. Despite recent advances in Pd(0)-catalyzed arylation at C(sp³)-H bonds,³ the scope of this reactivity remains limited and is mirrored by our incomplete mechanistic understanding of the C–H bond-cleaving event. Recent efforts by our group^{3j} as well as the groups of Clot and Baudoin^{3v} have led to a better understanding of this reactivity which has been proposed, based on density functional theory (DFT) calculations and KIE measurements, to proceed through

a CMD mechanism, similar to arylations at C(sp²)-H bonds. These findings highlight the possibility of a common mechanism for C–C bond formations at C–H bonds. Computational results point to the involvement of a three-center two-electron agostic interaction²² between the Pd(II) center and the C(sp³)-H bond being cleaved at the transition state (Figure 1).^{3j,v} These calculations also highlight the critical role of the basic additives in the CMD transition state of the reaction, typically in the form of carbonate or carboxylate derivatives. While computational

- (4) For selected examples of transition-metal-catalyzed transformations at C(sp³)-H bonds for C–C bond formation: Ruthenium (a) Pastine, S. J.; Gribkov, D. V.; Sames, D. *J. Am. Chem. Soc.* **2006**, *128*, 14220. (b) Jovel, I.; Prateetongkum, S.; Jackstell, R.; Vogl, N.; Weckbecker, C.; Beller, M. *Chem. Commun.* **2010**, 1956. Rhodium (c) Ishii, Y.; Chatani, N.; Kakiuchi, F.; Murai, S. *Organometallics* **1997**, *16*, 3615. (d) Chatani, N.; Asaumi, T.; Ikeda, T.; Yorimitsu, S.; Ishii, Y.; Kakiuchi, F.; Murai, S. *J. Am. Chem. Soc.* **2000**, *122*, 12882. (e) Kim, M.; Kwak, J.; Chang, S. *Angew. Chem., Int. Ed.* **2009**, *48*, 8935. Iridium (f) DeBoef, B.; Pastine, S. J.; Sames, D. *J. Am. Chem. Soc.* **2004**, *126*, 6556. (g) Tsuchikawa, K.; Kasagawa, M.; Endo, K.; Shibata, T. *Org. Lett.* **2009**, *11*, 1821. (h) Guo, Y.; Zhao, X.; Zhang, D.; Murahashi, S.-I. *Angew. Chem., Int. Ed.* **2009**, *48*, 2047. Titanium (i) Kubiak, R.; Prochnow, I.; Doye, S. *Angew. Chem., Int. Ed.* **2009**, *48*, 1153. (j) Bexrud, J. A.; Eisenberger, P.; Leitch, D. C.; Payne, P. R.; Schafer, L. L. *J. Am. Chem. Soc.* **2009**, *131*, 2116. (k) Kubiak, R.; Prochnow, I.; Doye, S. *Angew. Chem., Int. Ed.* **2010**, *49*, 2626. Tantalum (l) Herzon, S. B.; Hartwig, J. F. *J. Am. Chem. Soc.* **2007**, *129*, 6690. (m) Eisenberger, P.; Ayinla, R. O.; Lauzon, J. M. P.; Schafer, L. L. *Angew. Chem., Int. Ed.* **2009**, *48*, 8361. Platinum (n) Yang, S.; Li, Z.; Jian, X.; He, C. *Angew. Chem., Int. Ed.* **2009**, *48*, 3999. (o) Vadola, P. A.; Sames, D. *J. Am. Chem. Soc.* **2009**, *131*, 16525.
- (5) For selected examples of transition-metal-catalyzed transformations at C(sp³)-H bonds for C–X bond formation: (a) Kitajima, N.; Schwartz, J. J. *J. Am. Chem. Soc.* **1984**, *106*, 2220. (b) Olah, G. A.; Gupta, B.; Farina, M.; Felberg, J. D.; Ip, W. M.; Husain, A.; Karpeles, R.; Lammertsma, K.; Melhotra, A. K.; Trivedi, N. J. *J. Am. Chem. Soc.* **1985**, *107*, 7097. (c) Horváth, I. T.; Cook, R. A.; Millar, J. M.; Kiss, G. *Organometallics* **1993**, *12*, 8. (d) Giri, R.; Chen, X.; Yu, J.-Q. *Angew. Chem., Int. Ed.* **2005**, *44*, 2112. (e) Giri, R.; Chen, X.; Hao, X.-S.; Li, J.-J.; Liang, J.; Fan, Z.-P.; Yu, J.-Q. *Tetrahedron: Asymmetry* **2005**, *16*, 3502. (f) Hull, K. L.; Anani, W. Q.; Sanford, M. S. *J. Am. Chem. Soc.* **2006**, *128*, 7134. (g) Giri, R.; Wasa, M.; Breazzano, S. P.; Yu, J.-Q. *Org. Lett.* **2006**, *8*, 5685.
- (6) For selected examples of transition-metal-catalyzed transformations at C(sp³)-H bonds for C–B bond formation: (a) Chen, H.; Hartwig, J. F. *Angew. Chem., Int. Ed.* **1999**, *38*, 3391. (b) Chen, H.; Schlecht, S.; Semple, T. C.; Hartwig, J. F. *Science* **2000**, *287*, 1995. (c) Shimada, S.; Batsanov, A. S.; Howard, J. A. K.; Marder, T. B. *Angew. Chem., Int. Ed.* **2001**, *40*, 2168. (d) Lawrence, J. D.; Takahashi, M.; Bae, C.; Hartwig, J. F. *J. Am. Chem. Soc.* **2004**, *126*, 15334. (e) Murphy, J. M.; Lawrence, J. D.; Kawamura, K.; Incarvito, C.; Hartwig, J. F. *J. Am. Chem. Soc.* **2006**, *128*, 13684. (f) Olsson, V. J.; Szabó, K. J. *Angew. Chem., Int. Ed.* **2007**, *46*, 6891.
- (7) For an example of a transition-metal-catalyzed transformation at a C(sp³)-H bond for C–Si bond formation: Kakiuchi, F.; Tsuchiya, K.; Matsumoto, M.; Mizushima, E.; Chatani, N. *J. Am. Chem. Soc.* **2004**, *126*, 12792.
- (8) For selected examples of transition-metal-catalyzed transformations at C(sp³)-H bonds for C–O bond formation: (a) Heumann, A.; Reglier, M.; Waegell, B. *Angew. Chem., Int. Ed. Engl.* **1982**, *21*, 366. (b) Heumann, A.; Åkermarck, B. *Angew. Chem., Int. Ed. Engl.* **1984**, *96*, 443. (c) McMurry, J. E.; Koovsky, P. *Tetrahedron Lett.* **1984**, *25*, 4187. (d) Periana, R. A.; Taube, D. J.; Gamble, S.; Taube, H.; Satoh, T.; Fujii, H. *Science* **1998**, *280*, 560. (e) Lin, M.; Shen, C.; Garcia-Zayas, E. A.; Sen, A. *J. Am. Chem. Soc.* **2001**, *123*, 1000. (f) Dangel, B. D.; Johnson, J. A.; Sames, D. *J. Am. Chem. Soc.* **2001**, *123*, 8149. (g) Muehlhofer, M.; Strassner, T.; Herrmann, W. A. *Angew. Chem., Int. Ed.* **2002**, *41*, 1745. (h) Dick, A. R.; Hull, K. L.; Sanford, M. S. *J. Am. Chem. Soc.* **2004**, *126*, 2300. (i) Jones, C. J.; Taube, D.; Ziatdinov, V. R.; Periana, R. A.; Nielsen, R. J.; Oxgaard, J.; Goddard, W. A., III. *Angew. Chem., Int. Ed.* **2004**, *43*, 4626. (j) Desai, L. V.; Hull, K. L.; Sanford, M. S. *J. Am. Chem. Soc.* **2004**, *126*, 9542. (k) Chen, M. S.; White, M. C. *J. Am. Chem. Soc.* **2004**, *126*, 1346. (l) Giri, R.; Liang, J.; Lei, J.-G.; Li, J.-J.; Wang, D.-H.; Chen, X.; Nagggar, I. C.; Guo, C.; Foxman, B. M.; Yu, J.-Q. *Angew. Chem., Int. Ed.* **2005**, *44*, 7420. (m) Chen, M. S.; Prabakaran, N.; Labenz, N. A.; White, M. C. *J. Am. Chem. Soc.* **2005**, *127*, 6970. (n) Fraunhoffer, K. J.; Bachovchin, D. A.; White, M. C. *Org. Lett.* **2005**, *7*, 223. (o) Desai, L. V.; Malik, H. A.; Sanford, M. S. *J. Am. Chem. Soc.* **2006**, *8*, 1141. (p) Wang, D.-H.; Hao, X.-S.; Wu, D.-F.; Yu, J.-Q. *Org. Lett.* **2006**, *8*, 3387. (q) Lee, J. M.; Chang, S. *Tetrahedron Lett.* **2006**, *47*, 1375. (r) Fraunhoffer, K. J.; Prabakaran, N.; Sirois, L. E.; White, M. C. *J. Am. Chem. Soc.* **2006**, *128*, 9032. (s) Delcamp, J. H.; White, M. C. *J. Am. Chem. Soc.* **2006**, *128*, 15076. (t) Zhang, J.; Khaskin, E.; Anderson, N. P.; Zavalij, P. Y.; Vedernikov, A. N. *Chem. Commun.* **2008**, 3625. (u) Covell, D. J.; White, M. C. *Angew. Chem., Int. Ed.* **2008**, *47*, 6448. See also ref 2e.
- (9) For selected examples of transition-metal-catalyzed transformations at C(sp³)-H bonds for C–N bond formation: (a) Espino, C. G.; When, P. M.; Chow, J.; Du Bois, J. J. *J. Am. Chem. Soc.* **2001**, *123*, 6935. (b) Fraunhoffer, K. J.; White, M. C. *J. Am. Chem. Soc.* **2007**, *129*, 7274. (c) Du, H.; Yuan, W.; Zhao, B.; Shi, Y. *J. Am. Chem. Soc.* **2007**, *129*, 7496. (d) Wasa, M.; Yu, J.-Q. *J. Am. Chem. Soc.* **2008**, *130*, 14058. (e) Reed, S. A.; White, M. C. *J. Am. Chem. Soc.* **2008**, *130*, 3316. (f) Liu, G.; Yin, G.; Wu, L. *Angew. Chem., Int. Ed.* **2008**, *47*, 4733. (g) Wang, B.; Du, H.; Shi, Y. *Angew. Chem., Int. Ed.* **2008**, *47*, 8224. (h) Du, H.; Zhao, B.; Shi, Y. *J. Am. Chem. Soc.* **2008**, *130*, 8590. (i) Wu, L.; Qiu, S.; Liu, G. *Org. Lett.* **2009**, *11*, 2707. (j) Neumann, J. J.; Rakshit, S.; Dröge, T.; Glorius, F. *Angew. Chem., Int. Ed.* **2009**, *48*, 6892. (k) Reed, S. A.; Mazzotti, A. R.; White, M. C. *J. Am. Chem. Soc.* **2009**, *131*, 11701. (l) Rice, G. T.; White, M. C. *J. Am. Chem. Soc.* **2009**, *131*, 11707.
- (10) For an example of a transition-metal-catalyzed transformation at a C(sp³)-H bonds for C–S bond formation: Mukhopadhyay, S.; Bell, A. T. *Angew. Chem., Int. Ed.* **2003**, *42*, 2990.
- (11) For selected reviews on transition-metal-catalyzed transformations at acidic C(sp³)-H bonds: (a) Miura, M.; Nomura, M. *Top. Curr. Chem.* **2002**, *219*, 212. (b) Lloyd-Jones, G. C. *Angew. Chem., Int. Ed.* **2002**, *41*, 953. (c) Culkin, D. A.; Hartwig, J. F. *Acc. Chem. Res.* **2003**, *36*, 234. (d) Bellina, F.; Rossi, R. *Chem. Rev.* **2009**, *110*, 1082. (e) Johansson, C. C. C.; Colacot, T. J. *Angew. Chem., Int. Ed.* **2010**, *49*, 676.
- (12) For selected reviews on catalytic transformations at C(sp³)-H bonds: (a) Yu, J.-Q.; Giri, R.; Chen, X. *Org. Biomol. Chem.* **2006**, *4*, 4041. (b) Campos, K. R. *Chem. Soc. Rev.* **2007**, *36*, 1069. (c) Jazzar, R.; Hitec, J.; Renaudat, A.; Sofack-Kreutzer, J.; Baudoin, O. *Chem.-Eur. J.* **2010**, *16*, 2654. See also ref 11.
- (13) For selected general reviews on catalytic transformations at C–H bonds for the formation of C–C and C–X bonds: (a) Kakiuchi, F.; Chatani, N. *Adv. Synth. Catal.* **2003**, *345*, 1077. (b) *Handbook of C–H Transformations*; Dyker, G., Ed.; Wiley-VCH: Weinheim, 2005. (c) Godula, K.; Sames, D. *Science* **2006**, *312*, 67. (d) Dick, A. R.; Sanford, M. S. *Tetrahedron* **2006**, *62*, 2439. (e) Thansandote, P.; Lautens, M. *Chem.-Eur. J.* **2009**, *15*, 5974. (f) Zhang, M. *Adv. Synth. Catal.* **2009**, *351*, 2243. (g) Lyons, T. W.; Sanford, M. S. *Chem. Rev.* **2010**, *110*, 1147.

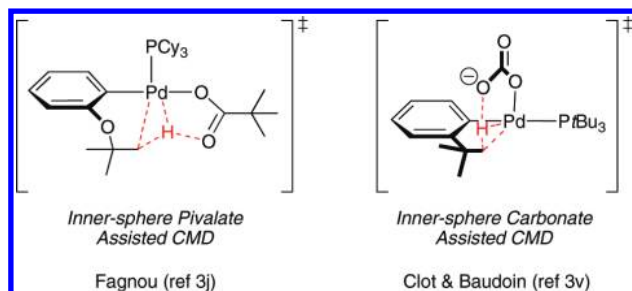


Figure 1. Transition states for concerted metalation–deprotonation (CMD) in Pd(0)/Pd(II)-catalyzed C(sp³)–H bond functionalization

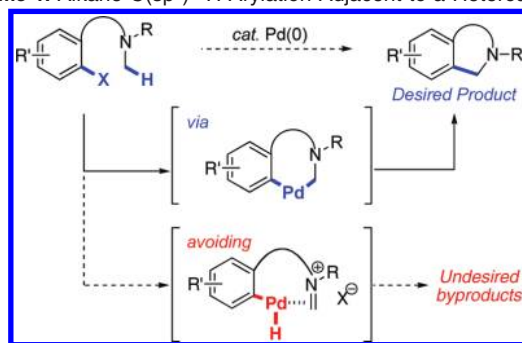
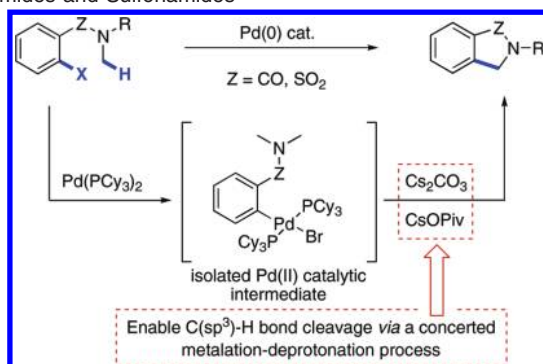
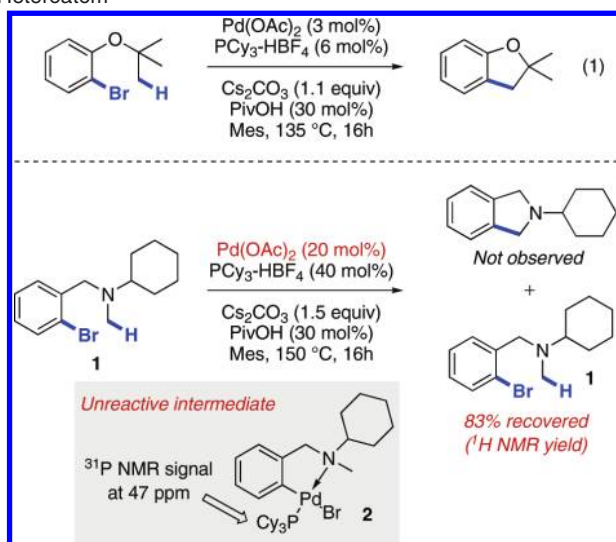
results accurately predict the reaction outcomes from the proposed CMD transition state, few experimental studies have been carried out to directly probe the mechanism of these transformations. Furthermore, theoretical calculations related to the mechanism of carbon–carbon bond formation at C–H bonds under Pd(0) catalysis heavily rely on the assumption of a Pd(0)/Pd(II) catalytic cycle being operative with C–H bond cleavage occurring at a Pd(II) species. However, the isolation of a Pd(II) catalytic intermediate and the direct observation of C–C bond formation *via* C–H bond cleavage from this intermediate have not been previously reported.

Examples of arylation at aliphatic positions adjacent to a heteroatom under Pd(0)/Pd(II) catalysis remain limited despite the general perception of these C–H bonds as “activated” toward transition-metal catalysis. Pioneering work by Dyker demonstrated the use of oxidative addition of an aryl-halide to

a Pd(0) catalyst as a tool to functionalize C(sp³)–H bonds adjacent to oxygen by effectively bringing the catalyst in close proximity to the aliphatic positions.^{3a} To our knowledge, little progress has since been reported for Pd(0)-catalyzed arylation at aliphatic positions adjacent to heteroatoms,²³ with no examples of reactivity at C(sp³)–H bonds adjacent to nitrogen being reported to date.^{12b,24} The apparent modest developments in this area of C(sp³)–H bond functionalization can be attributed to the α -heteroatom effect²⁵ and the intrinsic hurdle it poses to the desired reactivity. Indeed, heteroatom binding to Pd(II) through its lone pair and subsequent β -hydride elimination can lead to the overall unproductive dehalogenation of the starting material, a well documented process in Pd(0)/Pd(II) catalysis (Scheme 1).²⁶

Herein, we describe (1) the establishment of a Pd(0)-catalyzed intramolecular arylation reaction at aliphatic positions adjacent to a nitrogen atom in amides and sulfonamides, (2) the rare example of an isolated, catalytically active Pd(II) intermediate in Pd(0)-catalyzed C–C bond formation at nonacidic C(sp³)–H bonds, (3) mechanistic studies to evaluate the purpose of both

- (14) For selected reviews on catalytic transformations at C–H bonds for the formation of C–C bonds: (a) Dyker, G. *Angew. Chem., Int. Ed.* **1999**, *38*, 1698. (b) Rittling, V.; Sirlin, C.; Pfeffer, M. *Chem. Rev.* **2002**, *102*, 1731. (c) Goj, L. A.; Gunnoe, T. B. *Curr. Org. Chem.* **2005**, *9*, 671. (d) Daugulis, O.; Zaitsev, V. G.; Shabashov, D.; Pham, Q. N.; Lazareva, A. *Synlett* **2006**, 3382. (e) Alberico, D.; Scott, M. E.; Lautens, M. *Chem. Rev.* **2007**, *107*, 174. (f) Seregin, I. V.; Gevorgyan, V. *Chem. Soc. Rev.* **2007**, *36*, 1173. (g) Satoh, T.; Miura, M. *Chem. Lett.* **2007**, *36*, 200. (h) Campeau, L.-C.; Stuart, D. R.; Fagnou, K. *Aldrich. Chim. Acta* **2007**, *40*, 35. (i) Chen, X.; Engle, K. M.; Wang, D.-H.; Yu, J.-Q. *Angew. Chem., Int. Ed.* **2009**, *48*, 5094. (j) Daugulis, O.; Do, H.-Q.; Shabashov, D. *Acc. Chem. Res.* **2009**, *42*, 1074. (k) McGlacken, G. P.; Bateman, L. M. *Chem. Soc. Rev.* **2009**, *38*, 2447.
- (15) For selected reviews on palladium-catalyzed C–C bond formation at C(sp²)–H bonds: (a) Campeau, L.-C.; Fagnou, K. *Chem. Commun.* **2006**, 1253. (b) Li, B.-J.; Yang, S.-D.; Shi, Z.-J. *Synlett* **2008**, 949.
- (16) For selected reviews on ruthenium- or rhodium-catalyzed C–C bond formation at C(sp²)–H bonds: (a) Kakiuchi, F.; Murai, S. *Acc. Chem. Res.* **2002**, *35*, 826. (b) Lewis, J. C.; Bergman, R. G.; Ellman, J. A. *Acc. Chem. Res.* **2008**, *41*, 1013. (c) Colby, D. A.; Bergman, R. G.; Ellman, J. A. *Chem. Rev.* **2010**, *110*, 624.
- (17) For selected reviews on transformations at C(sp³)–H bonds involving an outer-sphere mechanism: (a) Davies, H. M. L.; Beckwith, R. E. *J. Chem. Rev.* **2003**, *103*, 2861. (b) Davies, H. M. L.; Loe, Ø. *Synthesis* **2004**, 2595. (c) Davies, H. M. L.; Manning, J. R. *Nature* **2008**, *451*, 417. (d) Díaz-Requejo, M. M.; Pérez, P. J. *Chem. Rev.* **2008**, *108*, 3379. (e) Zalatan, D. N.; Du Bois, J. *Top. Curr. Chem.* **2009**, 1436. (f) Collet, F.; Dodd, R. H.; Dauban, P. *Chem. Commun.* **2009**, 5061. (g) Doyle, M. P.; Duffy, R.; Ratnikov, M.; Zhou, L. *Chem. Rev.* **2010**, *110*, 704. See also ref 13d.
- (18) For selected examples of stoichiometric inner-sphere reactions at C(sp³)–H bonds: (a) Shilov, A. E.; Shteinman, A. A. *Coord. Chem. Rev.* **1977**, *24*, 97, and references therein. (b) Labinger, J. A. *J. Mol. Catal. A: Chem.* **2004**, *220*, 27, and references therein.
- (19) For selected reviews related to the mechanism of transformations at C(sp³)–H bonds: (a) Ryabov, A. D. *Chem. Rev.* **1990**, *90*, 403. (b) Shilov, A. E.; Shul'pin, G. B. *Chem. Rev.* **1997**, *97*, 2879. (c) Stahl, S. S.; Labinger, J. A.; Bercaw, J. E. *Angew. Chem., Int. Ed.* **1998**, *37*, 2180. (d) Crabtree, R. H. *J. Chem. Soc., Dalton Trans.* **2001**, 2437. (e) Labinger, J. A.; Bercaw, J. E. *Nature* **2002**, *417*, 507. (f) Crabtree, R. H. *J. Organomet. Chem.* **2004**, *689*, 4083. (g) Lersch, M.; Tilstet, M. *Chem. Rev.* **2005**, *105*, 2471.
- (20) For selected reviews: (a) Biswas, B.; Sugimoto, M.; Sakaki, S. *Organometallics* **2000**, *19*, 3895. (b) Pascual, S.; de Mendoza, P.; Echavarren, A. M. *Org. Biomol. Chem.* **2007**, *5*, 2727. (c) Boutadla, Y.; Davies, D. L.; Macgregor, S. A.; Poblador-Bahamonde, A. I. *Dalton Trans.* **2009**, 5820. (d) Balcells, D.; Clot, E.; Eisenstein, O. *Chem. Rev.* **2010**, *110*, 749.
- (21) For selected references supporting a concerted metalation–deprotonation pathway in transition-metal-catalyzed transformations at C(sp²)–H bonds: (a) Mota, A. J.; Dedieu, A.; Bour, C.; Suffert, J. *J. Am. Chem. Soc.* **2005**, *127*, 7171. (b) Davies, D. L.; Donald, S. M. A.; Macgregor, S. A. *J. Am. Chem. Soc.* **2005**, *127*, 13754. (c) García-Cuadrado, D.; Braga, A. A. C.; Maseras, F.; Echavarren, A. M. *J. Am. Chem. Soc.* **2006**, *128*, 1066. (d) Davies, D. L.; Donald, S. M. A.; Al-Duaij, O.; Macgregor, S. A.; Pölleth, M. *J. Am. Chem. Soc.* **2006**, *128*, 4210. (e) Lafrance, M.; Rowley, C. N.; Woo, T. K.; Fagnou, K. *J. Am. Chem. Soc.* **2006**, *128*, 8754. (f) Lafrance, M.; Fagnou, K. *J. Am. Chem. Soc.* **2006**, *128*, 16496. (g) García-Cuadrado, D.; de Mendoza, P.; Braga, A. A. C.; Maseras, F.; Echavarren, A. M. *J. Am. Chem. Soc.* **2007**, *129*, 6880. (h) Ackermann, L.; Vicente, R.; Althammer, A. *Org. Lett.* **2008**, *10*, 2299. (i) Caron, L.; Campeau, L.-C.; Fagnou, K. *Org. Lett.* **2008**, *10*, 4533. (j) Gorelsky, S. I.; Lapointe, D.; Fagnou, K. *J. Am. Chem. Soc.* **2008**, *130*, 10848. (k) Lafrance, M.; Lapointe, D.; Fagnou, K. *Tetrahedron* **2008**, *64*, 6015. (l) Pascual, S.; de Mendoza, P.; Braga, A. A. C.; Maseras, F.; Echavarren, A. M. *Tetrahedron* **2008**, *64*, 6021. (m) Özdemir, I.; Demir, S.; Çetinkaya, B.; Gourelaouen, C.; Maseras, F.; Bruneau, C.; Dixneuf, P. H. *J. Am. Chem. Soc.* **2008**, *130*, 1156. (n) Liégault, B.; Lapointe, D.; Caron, L.; Vlassova, A.; Fagnou, K. *J. Org. Chem.* **2009**, *74*, 1826. (o) Liégault, B.; Petrov, I.; Gorelsky, S. I.; Fagnou, K. *J. Org. Chem.* **2010**, *75*, 1047.
- (22) For a review on agostic interactions in transition metal compounds: Brookhart, M.; Green, M. L. H.; Parkin, G. *Proc. Natl. Acad. Sci. U.S.A.* **2007**, *104*, 6908.
- (23) For examples utilizing Dyker's methodology: (a) Kim, H. S.; Gowrisankar, S.; Kim, S. H.; Kim, J. N. *Tetrahedron Lett.* **2008**, *49*, 3858. (b) Suau, R.; López-Romero, J. M.; Rico, R. *Tetrahedron Lett.* **1996**, *37*, 9357.
- (24) For selected examples of transition-metal catalyzed transformations at C(sp³)–H bonds adjacent to nitrogen for the formation of C–C bonds, see ref 4a,d,f. For metal-catalyzed transformations proceeding *via* a radical mechanism: (a) Baslé, O.; Li, C.-J. *Org. Lett.* **2008**, *10*, 3661. (b) Yoshikai, N.; Mieczkowski, A.; Matsumoto, A.; Ilies, L.; Nakamura, E. *J. Am. Chem. Soc.* **2010**, *132*, 5568.
- (25) For a review: Murahashi, S.-I.; Takaya, H. *Acc. Chem. Res.* **2000**, *33*, 225.
- (26) This pathway is indeed a well-known mechanism for the generation of Pd(0) from the reaction of Pd(II) precatalysts with triethylamine in other traditional cross-coupling reactions. As well, the undesired dehalogenation of aryl halides *via* this mechanism has been previously documented in the development of palladium-catalyzed aryl amination reactions as well as other palladium-catalyzed cross-coupling processes. See: (a) Brenda, M.; Knebelkamp, A.; Greiner, A.; Heitz, W. *Synlett* **1991**, 809. (b) Guram, A. S.; Rennels, R. A.; Buchwald, S. L. *Angew. Chem., Int. Ed. Engl.* **1995**, *34*, 1348. (c) Hartwig, J. F.; Richards, S.; Barañano, D.; Paul, F. *J. Am. Chem. Soc.* **1996**, *118*, 3626.

Scheme 1. Alkane C(sp³)–H Arylation Adjacent to a Heteroatom**Scheme 2.** Pd(0)-Catalyzed Arylation at C(sp³)–H Bonds Adjacent to Amides and Sulfonamides**Scheme 3.** Initial Investigation of Alkane Arylation Adjacent to a Heteroatom

the pivalate and carbonate bases in the CMD mechanism, (4) computational results to further elucidate the roles of both bases in C(sp³)–H bond cleavage, and (5) kinetic studies to gain insight into the factors that govern catalysis (Scheme 2).

2. Results and Discussion

2.1. Reaction Development and Scope. Inspired by our report of an intramolecular Pd(0)-catalyzed alkane arylation to generate 2,2-dialkylidihydrobenzofurans (Scheme 3, eq 1),^{3j} a preliminary screening of reaction conditions for the cyclization of amine **1** led to the recovery of starting material. Increasing the catalyst loading to 20 mol % Pd(OAc)₂ also did not afford the desired product, and starting material **1** was recovered in 83% yield. The latter result suggests that the proportional decrease in starting material recovery with a higher catalyst loading might

arise from the formation of a problematic unreactive intermediate **2** (Scheme 3). Indeed, a ³¹P NMR spectrum of the crude reaction mixture reveals a signal at 47 ppm, correlating with previous literature reports for similar complexes.²⁷

To further probe the lack of reactivity with amine **1**, one-pot reactions were performed with either amine **1** or **4** in the presence of ether **3** in a 1:1 ratio. Ether **3** was chosen as a probe for catalyst availability as it is a highly reactive substrate toward alkane arylation (Scheme 4).²⁸ While reaction of **3** in the presence of **1** led to starting material recovery (eq 2), reactivity was completely restored in the presence of amine **4** (eq 3). This supports the hypothesis of catalyst sequestration in the former reaction through the formation of intermediate **2** where the nitrogen lone pair of the substrate coordinates the Pd(II) center, inhibiting further reactivity. Similar experiments performed with amine **1** (or **4**) in the presence of ether **6** (eqs 4 and 5), containing an electron-withdrawing group on the arene ring, led to the same conclusion as to the problematic formation of palladacycle **2**. Nonetheless, in this situation some product of alkane arylation **7** is observed in the presence of amine **1** (eq 4), highlighting the greater ease of oxidative insertion of electron-deficient aryl bromides to Pd(0).

Hypothesizing that a less Lewis basic nitrogen was required to avoid the undesired formation of palladacycle **2**, we chose amide **8** as a substrate for alkane arylation adjacent to a heteroatom. A screening of reaction conditions (*vide infra*) uncovered that amide **8** reacts smoothly to afford the product of alkane arylation **9** (Scheme 5).

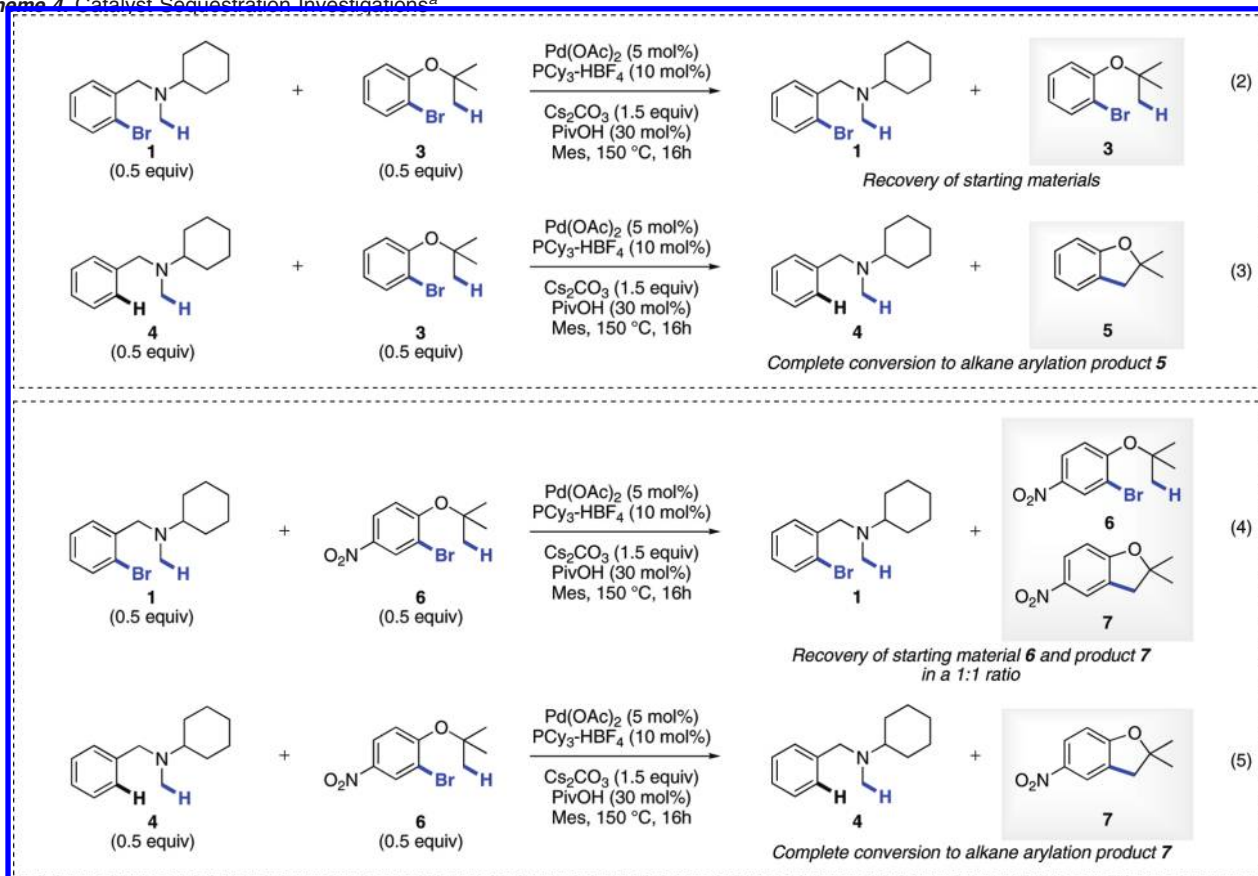
Over the course of these studies, the base demonstrated an important influence on the outcome of the reaction. Similar to previous reports,^{3j,ab,21h,i,k,o} both the carbonate and the pivalate additives appear to play an important role (Table 1). When the reaction was carried out in the presence of a stoichiometric amount of Cs₂CO₃, an insoluble base under the reaction conditions, 15% conversion to product was observed (Table 1, entry 1). Changing the base to the more soluble CsOPiv led to 6% conversion (entry 2). However, when a stoichiometric quantity of a carbonate base in combination with a catalytic or stoichiometric amount of pivalate was used, complete conversion of starting material was obtained with the desired product isolated in yields greater than 83% (entries 4–5). In comparison, the use of cesium carbonate as the stoichiometric base in conjunction with a catalytic amount of acetic acid leads to a significantly decreased product yield (entry 3).²⁹

A further screen of alkali carbonates showed a surprising counterion effect for the alkane arylation of *N*-methanilamides (Table 2). While the reaction with Na₂CO₃ provides no product (Table 2, entry 1), the reaction with K₂CO₃ gives incomplete conversions and significant amounts of dehalogenated starting material as a reaction byproduct (entry 2). Rb₂CO₃ was found to be the optimal base for the cyclization of 2-bromoaryl amides. The use of this base was particularly successful in cases where

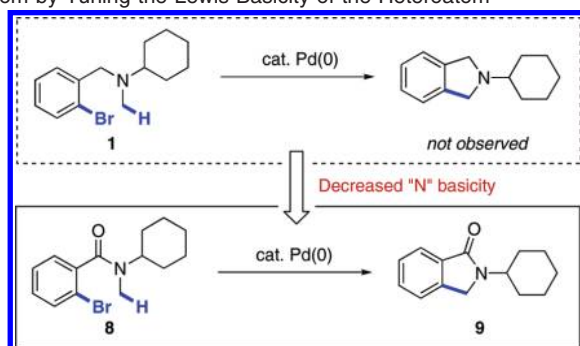
(27) A signal (s) at 45 ppm was observed for the corresponding *N*-(2-bromobenzyl)-*N*-dimethylamine derived complex, see: Bedford, R. B.; Cazin, C. S. J. *Organometallics* **2003**, *22*, 987.

(28) Under reaction conditions previously reported by our group for alkane arylation of these types of ethers, substrate **3** is converted to 2,2-dialkylidihydrobenzofuran **5** in 97% yield and **6** is converted to **7** in 91% yield (see ref 3j).

(29) The nature of the intrinsic difference in reactivity of pivalate vs acetate additives remains elusive at this time. The significant decrease in yield when acetic acid is used instead of pivalic acid as an additive in Pd(0)-catalyzed transformations at C–H bonds has been previously observed (see refs 3j and 21f,k). Efforts are underway to further understand these observations.

Scheme 4. Catalyst Sequestration Investigations^a

^a Reaction outcomes were determined by GC/MS using 1,3,5-trimethoxybenzene as an internal standard. Formation of **5** and **7** were confirmed by ¹H NMR.

Scheme 5. Arylation at a C(sp³)–H Bond Adjacent to a Nitrogen Atom by Tuning the Lewis Basicity of the Heteroatom

less sterically demanding substituents were present on the amide nitrogen to minimize the undesired formation of dehalogenated starting material. Indeed, lactam **11** was isolated in 56% yield when Rb_2CO_3 was chosen as the source of base compared to 48% for Cs_2CO_3 (entries 3 and 4).

The formation of product **13** from amide **12** was studied with a variety of ligands possessing different steric and electronic properties (Table 3). While $\text{PCy}_3\cdot\text{HBF}_4$ was found to be the optimal ligand for good product yields (entry 1), interesting steric and electronic trends were uncovered. The reaction appears to be very sensitive to the steric bulk of the ligand. Indeed, minimal product formation is observed in the presence of $\text{PtBu}_3\cdot\text{HBF}_4$ compared to the 76% yield of **13** when $\text{PCy}_3\cdot\text{HBF}_4$ is used (entries 1–2). In addition, the significant difference in yield for reactions employing electron-poor and electron-rich

Table 1. Effect of the Base and the Additive on the Alkane Arylation of *N*-Methylamides

Reaction (1): 2-bromo-N-methylbenzylamine (8) $\xrightarrow[\text{Base} (1.5 \text{ equiv.}), \text{Additive} (x \text{ mol\%}), \text{Mesitylene}, 150^\circ\text{C}, 16\text{h}]{\text{Pd}(\text{OAc})_2 (5 \text{ mol\%}), \text{PCy}_3\cdot\text{HBF}_4 (10 \text{ mol\%})}$ 2-bromo-N-methylbenzylamine (8). not observed.

Reaction (2): 2-bromo-N-methylbenzylamine (8) $\xrightarrow[\text{Base} (1.5 \text{ equiv.}), \text{Additive} (x \text{ mol\%}), \text{Mesitylene}, 150^\circ\text{C}, 16\text{h}]{\text{Pd}(\text{OAc})_2 (5 \text{ mol\%}), \text{PCy}_3\cdot\text{HBF}_4 (10 \text{ mol\%})}$ 2-bromo-N-methylbenzylamine (8). not observed.

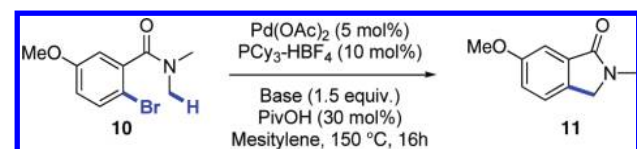
Reaction (3): 2-bromo-N-methylbenzylamine (8) $\xrightarrow[\text{Base} (1.5 \text{ equiv.}), \text{Additive} (x \text{ mol\%}), \text{Mesitylene}, 150^\circ\text{C}, 16\text{h}]{\text{Pd}(\text{OAc})_2 (5 \text{ mol\%}), \text{PCy}_3\cdot\text{HBF}_4 (10 \text{ mol\%})}$ 2-bromo-N-methylbenzylamine (8). not observed.

Entry	Base	Additive	Yield (%) ^a
1	Cs_2CO_3	none	14 ^b
2	CsOPiv	none	5 ^b
3	Cs_2CO_3	AcOH (30 mol %)	27 ^b
4	Cs_2CO_3	PivOH (30 mol %)	83
5	Cs_2CO_3	CsOPiv (110 mol %)	88

^a Isolated yields. ^b Determined by GC-MS using 1,3,5-trimethoxybenzene as an internal standard.

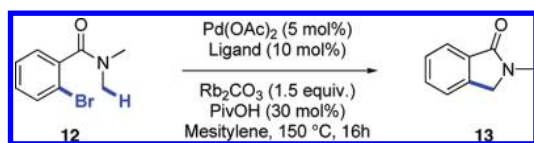
triarylphosphines demonstrates the importance of employing electron-rich ligands to promote product formation (entries 5–6).

Illustrative examples of the scope of the reaction with respect to substitution on both the aliphatic and aromatic portions of the amide are shown in Table 4. 2-Bromo-*N,N*-dimethylbenzamide **12** reacts smoothly to give product **13** in 76% isolated yield (Table 4, entry 1). The alkane arylation of more sterically encumbered cyclohexyl and *iso*-butyl substituted *N*-methylamides proceeds in good yields, affording products **9** and **15** in 83% and 68% yield respectively (entries 2 and 3). Exclusive selectivity is observed for arylation at methyl over methylene or methyne C(sp³)–H bonds, which correlates with previous experimental and computational results.^{3j,v} The reaction of **16**, possessing a remote phenyl functionality, gives rise to isoin-

Table 2. Optimization of the Source of Alkali Carbonates in Alkane Arylation of *N*-Methylamides

Entry	Base	Yield (%) ^a
1	Na ₂ CO ₃	0 ^b
2	K ₂ CO ₃	31
3	Rb₂CO₃	56
4	Cs ₂ CO ₃	48

^a Isolated yields. ^b Determined by GC-MS using 1,3,5-trimethoxybenzene as an internal standard.

Table 3. Effect of the Ligand on the Alkane Arylation of *N*-Methylamides

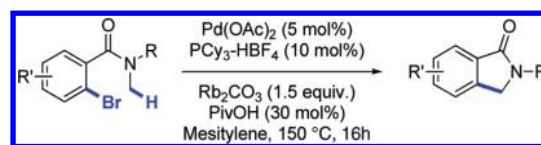
Entry	Ligand	Yield (%) ^a
1	PCy₃·HBF₄	76^b
2	PrBu ₃ ·HBF ₄	5
3	PrBu ₂ Me·HBF ₄	13
4	CyJohnPhos ^c	17
5	P(<i>p</i> -F-C ₆ H ₄) ₃	9
6	P(<i>p</i> -OMe-C ₆ H ₄) ₃	24

^a Determined by GC-MS using 1,3,5-trimethoxybenzene as an internal standard. ^b Isolated yield. ^c CyJohnPhos = 2-(Dicyclohexylphosphino)biphenyl.

doline **17** albeit in lower yield (entry 4). On the aromatic portion of the amide, the presence of an electron-donating group leads to slightly attenuated reactivity. For example, methoxy-substituted 2-bromoaryl amides **10** and **18** generate products **11** and **19** in 56% and 44% yield respectively (entries 5 and 6). Fluorinated arene **20** also reacts well, yielding product **21** in 70% (entry 7).

The functionalization of C–H bonds adjacent to other electron-poor nitrogen-containing functional groups was also investigated. Sulfonamides were found to be compatible substrates for this transformation when Cs₂CO₃ was used as a base (Table 5). Indeed, aryl bromide **22** provides product **23** in 62% yield (entry 1). Other simple alkane substituents on the sulfonamide are tolerated under the reaction conditions as exemplified by *n*-butyl-substituted sulfonamide **24** and dimethylsulfonamide **26** (entries 2 and 3). The presence of functional groups such as an ether (entry 4) and a TIPS-protected alcohol (entry 5) does not hinder product formation as **29** and **31** are obtained in moderate yields (59% and 47% respectively). Finally, Lewis basic functional groups such as amines are well tolerated as exemplified by the formation of product **33** in 71% yield (entry 6).

An intramolecular competition reaction was designed to probe the preference of the catalyst system for reactivity at sp² vs sp³ C–H bonds. When 2-bromo-*N*-methyl-*N*-phenylbenzamide **34** was exposed to the standard reaction conditions for arylation at aliphatic positions, exclusive selectivity for reaction at the arene C–H bond was observed, with product **35** being obtained in 88% yield (Scheme 6). A similar result was obtained for the corresponding sulfonamide **36**, which exclusively gave the product of direct arylation **37** in 83% yield. The complete

Table 4. Scope of the Intramolecular Alkane Arylation of *N*-Methylamides^a

Entry	Starting Material	Product	Yield (%) ^a
1			76
2			83
3			68
4			37
5			56
6			44
7			70

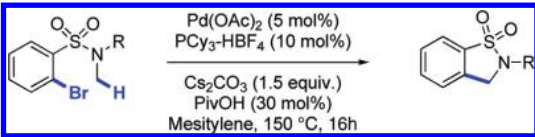
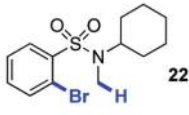
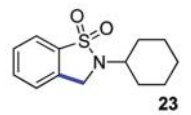
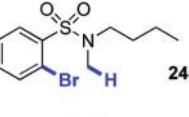
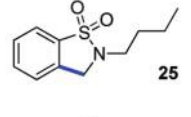

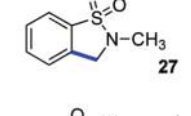
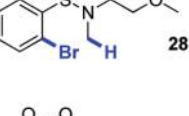
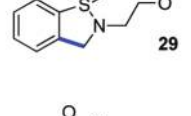
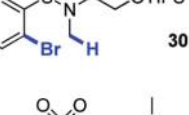
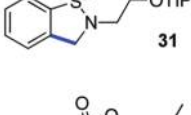
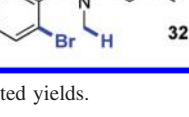
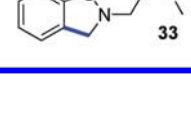
^a Isolated yields.

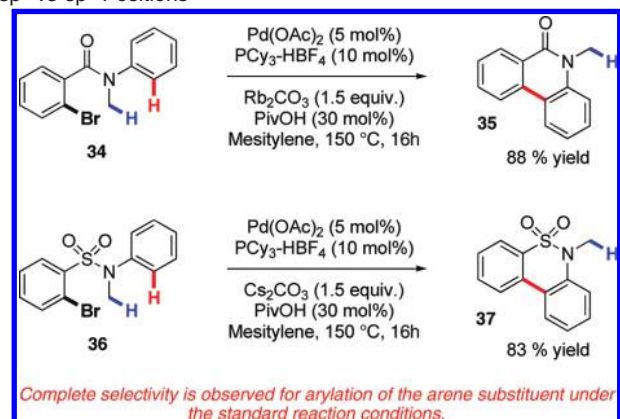
selectivity for C(sp²)-H arylation, despite the formation of a seven-membered palladacycle in this reaction pathway, compared to alkane arylation *via* a six-membered palladacycle, is dictated by more facile catalyst–substrate interactions through the π -system of the arene.

2.2. Mechanistic Studies. Initial computational evaluations of intramolecular Pd(0)-catalyzed alkane arylation reactions have begun to shed light on the mechanism of this reaction.^{3j,v} Although computational results correlate with experimental observations, little direct experimental evidence pertaining to the mechanism of C–H bond cleavage exists. Such mechanistic knowledge is required to facilitate further reaction development and catalyst design in this expanding area of research. To this effect, both mechanistic and kinetic experiments were devised to further our awareness of the parameters that guide reactivity in arylation reactions at aliphatic positions adjacent to heteroatoms.

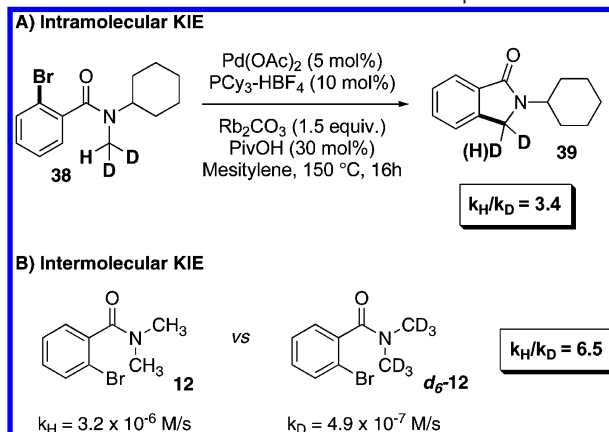
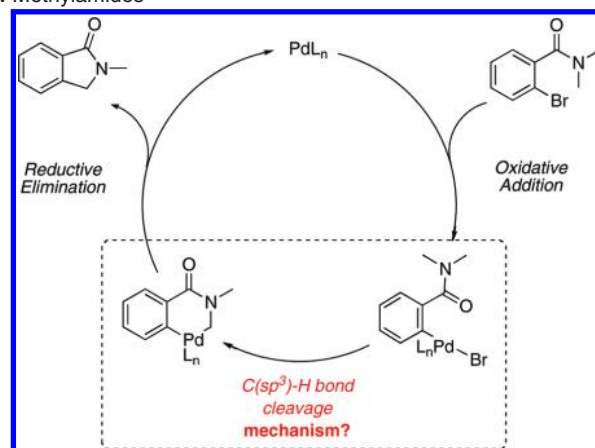
2.2.1. Kinetic Isotope Effect. An intramolecular kinetic isotope effect (KIE) study was conducted with substrate **38**, designed to observe the preference of the catalyst for C–H(D) bond cleavage without the bias of potential amide rotamers

Table 5. Scope of the Intramolecular Alkane Arylation of *N*-Methylsulfonamides

			
Entry	Starting Material	Product	Yield (%) ^a
1			62
2			82
3			52
4			59
5			47
6			71

^a Isolated yields.**Scheme 6.** Intramolecular Competition for Preferential Arylation at *sp*² vs *sp*³ Positions

(Scheme 7A).³⁰ The k_H/k_D value of 3.4 is indicative of a kinetically significant C–H bond-cleaving reaction step. To determine the importance of C–H bond cleavage in the overall reaction rate, an intermolecular KIE experiment was also carried out (Scheme 7B). A side-by-side comparison of reaction rates for 2-bromo-*N,N*-dimethylbenzamide **12** and *d*₆-2-bromo-*N,N*-dimethylbenzamide **d₆-12** led to a k_H/k_D value of 6.5 indicating

Scheme 7. Intra- and Intermolecular Kinetic Isotope Effects**Scheme 8.** General Catalytic Cycle for the Alkane Arylation of *N*-Methylamides

that the C–H(D) bond is cleaved during the rate-determining step of the reaction.^{31,32}

2.2.2. Isolation and Characterization of a Catalytically Competent Pd(II) Intermediate. The catalytic cycle for alkane arylation can be simplified to three steps: (1) oxidative addition of the aryl bromide to the Pd(0) catalyst, (2) C–H bond cleavage, and (3) reductive elimination of the desired product from the Pd(II) intermediate to regenerate the Pd(0) species (Scheme 8). Oxidative addition of aryl halides to Pd(0)-phosphine complexes and reductive elimination from Pd(II) complexes to form carbon–carbon bonds are well documented reactions whose mechanisms have been extensively studied.^{33,34} However, little experimental work has been done concerning

(31) The larger KIE value for intermolecular *vs* intramolecular competitions is atypical and is not fully understood at this time although errors on side-by-side intermolecular competitions are intrinsically larger due to the nature of the experiment. In any case, the conclusion of a rate-limiting C–H bond cleaving event remains.

(32) See Supporting Information for further details on kinetic experiments.

(33) For selected mechanistic studies on oxidative addition of Pd(0) to aryl halides: (a) Amatore, C.; Pflüger, F. *Organometallics* **1990**, *9*, 2276. (b) Hartwig, J. F.; Frédéric, P. *J. Am. Chem. Soc.* **1995**, *117*, 5373. (c) Amatore, C.; Bucaille, A.; Fuxa, A.; Jutand, A.; Meyer, G.; Ntepe, A. N. *Chem.–Eur. J.* **2001**, *7*, 2134. (d) Amatore, C.; Jutand, A.; Thuilliez, A. *J. Organomet. Chem.* **2002**, *643–644*, 416. (e) Barrios-Landeros, F.; Hartwig, J. F. *J. Am. Chem. Soc.* **2005**, *127*, 6944. (f) Barrios-Landeros, F.; Carrow, B. P.; Hartwig, J. F. *J. Am. Chem. Soc.* **2008**, *130*, 5842. (g) Barrios-Landeros, F.; Carrow, B. P.; Hartwig, J. F. *J. Am. Chem. Soc.* **2009**, *131*, 8141, and references therein.

(34) For selected mechanistic studies on reductive elimination from C–C bond formation: (a) Culkin, D. A.; Hartwig, J. F. *Organometallics* **2004**, *23*, 3398. (b) Racowski, J. M.; Dick, A. R.; Sanford, M. S. *J. Am. Chem. Soc.* **2009**, *131*, 10974.

(30) Signals for both amide conformations do not coalesce even at 120 °C on the ¹H NMR time scale.

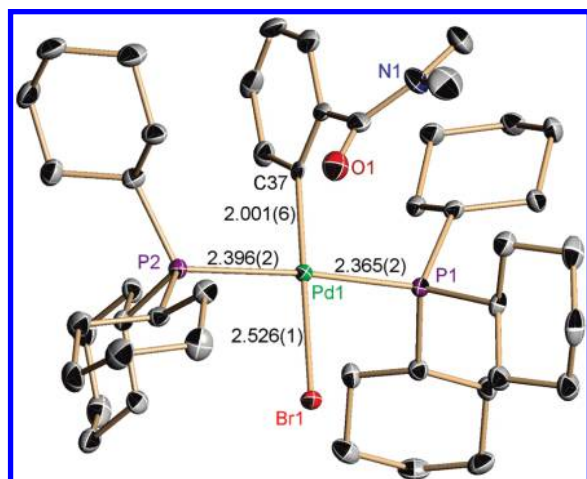
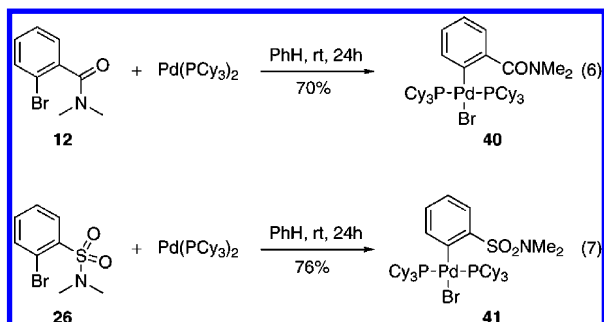


Figure 2. ORTEP plot of [(PCy₃)₂Pd(C₆H₄CONMe₂)(Br)] **40**. All H atoms have been omitted for clarity. Anisotropic displacement ellipsoids are shown at the 50% probability level. Selected bond lengths (Å) are indicated on the diagram.

the mechanism of C–H bond cleavage at aliphatic positions as well as the role of the bases involved in this elementary reaction step.

To examine this catalytic step, Pd(II) intermediate **40** resulting from oxidative insertion of 2-bromo-*N,N*-dimethylbenzamide **12** to L_nPd(0) was prepared. Reaction of 1.5 equiv of **12** with Pd(PCy₃)₂ in benzene at room temperature for 24 h led to the isolation of air-stable Pd(II) complex **40** in 70% yield (eq 6).³⁵ Similarly, the Pd(II) intermediate **41**, resulting from oxidative insertion of Pd(PCy₃)₂ to 2-bromo-*N,N*-dimethylbenzenesulfonamide **26**, was also prepared in 76% yield (eq 7). The structure of **40** was confirmed by X-ray crystallography and revealed a four-coordinate square planar complex containing two *trans* PCy₃ ligands (Figure 2). No significant interactions between the amide moiety and the Pd(II) center are present in the structure as the distances between Pd(1) and O(1) or N(1) are 3.09 and 4.50 Å respectively.



Prior to probing the mechanism of C–H bond cleavage with [(PCy₃)₂Pd(C₆H₄CONMe₂)(Br)] **40**, its nature as a catalytically relevant intermediate was first established to shed any potential doubt that it may represent an off-cycle unreactive catalytic species. To this effect, 2-bromo-*N,N*-dimethylbenzamide **12** was subjected to the standard reaction conditions, replacing Pd(OAc)₂ (5 mol %) and PCy₃·HBF₄ (10 mol %) with [(PCy₃)₂Pd(C₆H₄CONMe₂)(Br)] **40** (5 mol %). The product of alkane arylation **13** was obtained in 67% yield, compared to 76% under

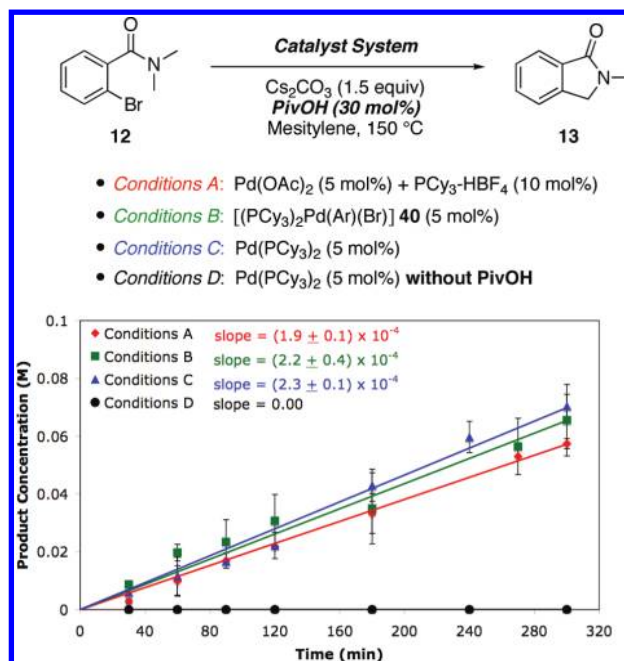
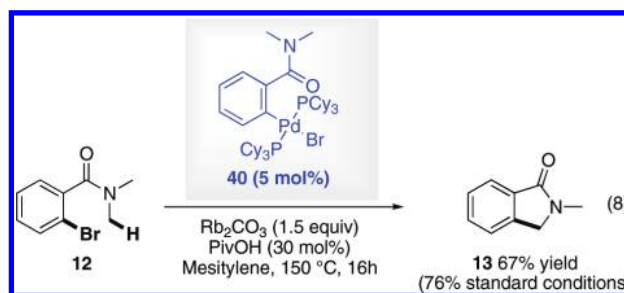


Figure 3. Initial formation of product **13** over time under different catalytic conditions: Pd(OAc)₂ (5 mol %) + PCy₃·HBF₄ (10 mol %) (Conditions A, red ♦), [(PCy₃)₂Pd(C₆H₄CONMe₂)(Br)] **40** (5 mol %) (Conditions B, green ■), Pd(PCy₃)₂ (5 mol %) (Conditions C, blue ▲) and Pd(PCy₃)₂ (5 mol %) without pivalic acid (Conditions D, black ●). The data points for product concentrations are the average of two runs and were determined by GC/MS using 1,3,5-trimethoxybenzene as an internal standard.

the standard reaction conditions, indicating that **40** is a catalyst precursor for the reaction (eq 8).



2.2.3. Comparative Reaction Kinetics for Different Catalyst Systems. The kinetic competence of [(PCy₃)₂Pd(C₆H₄CONMe₂)(Br)] **40**, as well as other Pd catalyst systems, for product formation was evaluated by following the reaction kinetics. The appearance of product over time was monitored by GC/MS using 1,3,5-trimethoxybenzene as an internal standard.³² Comparable rates of product formation were observed using three catalyst systems (Figure 3): the standard catalyst combination of Pd(OAc)₂ (5 mol %) and PCy₃·HBF₄ (10 mol %) (Conditions A), [(PCy₃)₂Pd(C₆H₄CONMe₂)(Br)] **40** (5 mol %) (Conditions B), and the commercially available Pd(0) catalyst Pd(PCy₃)₂ (5 mol %) (Conditions C). These comparable rates indicate the absence of a catalyst initiation period to generate Pd(0) from Pd(OAc)₂ under the standard reaction conditions (Conditions A) since rates of catalysis are comparable to those when Pd(0) systems are used (Conditions C). Moreover, these results demonstrate the ability of [(PCy₃)₂Pd(C₆H₄CONMe₂)(Br)] **40** to rapidly generate the active catalytic species for the CMD reaction step. A control reaction using Pd(PCy₃)₂ in the absence of a pivalate source (Conditions D) emphasizes once again the crucial role of this base for catalysis to occur.

(35) Stambuli, J. P.; Incarvito, C. D.; Bühl, M.; Hartwig, J. F. *J. Am. Chem. Soc.* **2004**, *126*, 1184.

Table 6. Stoichiometric Studies with [(PCy₃)₂Pd(Ar)(Br)] **40** and **41** To Probe the Role of Pivalate and Carbonate Bases in the CMD Pathway

<p>40 (Z = CO) 41 (Z = SO₂)</p> <p>Base (10 equiv) Additive (3 equiv) Mesitylene, 150 °C, 4 h</p> <p>13 (Z = CO) 27 (Z = SO₂)</p>			
Entry	Base	Additive	Yield (%) ^a
1	none	none	0
2	Cs ₂ CO ₃	none	0
3	CsOPiv	none	28
4	Cs ₂ CO ₃	CsOPiv	96
5	none	none	0
6	Cs ₂ CO ₃	none	7
7	CsOPiv	none	35
8	Cs ₂ CO ₃	CsOPiv	80

^a Determined by ¹H NMR using 1,3,5-trimethoxybenzene as an internal standard.

2.2.4. Stoichiometric Mechanistic Studies with [(PCy₃)₂Pd(Ar)(Br)] **40 and **41**.** To evaluate the role of both the pivalate and carbonate bases in the proposed concerted metalation–deprotonation (CMD) pathway for C(sp³)–H bond cleavage, stoichiometric studies with [(PCy₃)₂Pd(Ar)(Br)] **40** and **41** were carried out. Complexes **40** and **41** were chosen since they allow for a direct probe of the C–H bond cleaving step. The results of these stoichiometric studies, performed in mesitylene at 150 °C for 4 h with various bases and additives, are highlighted in Table 6.

Minimal or no product formation is observed in the absence of both forms of base (entries 1 and 5) as well as with the use of a strong carbonate base (entries 2 and 6). The stoichiometric reaction of complex **40** and **41** with CsOPiv generates products **13** and **27** in low yields (28% and 35% respectively) (entries 3 and 7). These results correlate with those reported in catalytic studies (Table 1). However, the modest reactivity observed with CsOPiv in the presence of *stoichiometric* palladium leads us to further examine our working hypothesis for the combined use of catalytic pivalate and stoichiometric carbonate in these reactions.^{21f} The use of both bases in *catalytic* transformations at C–H bonds that proceed *via* a CMD transition state has been rationalized by the requirement for a soluble basic species responsible for deprotonation (pivalate) and an insoluble proton sink responsible for sequestration of H⁺ and pivalate regeneration (carbonate). The latter should therefore not be required for product formation under *stoichiometric* conditions. Finally, the reaction of [(PCy₃)₂Pd(Ar)(Br)] **40** and **41** with Cs₂CO₃ (10.0 equiv) and CsOPiv (3.0 equiv) in mesitylene at 150 °C for 4 h gave 96% and 80% yields of alkane arylation products **13** and **27** respectively (entries 4 and 8).³⁶ These results not only support the required combination of carbonate and pivalate for productive reactions (see Table 1) but also underline the complexity of the role(s) played by these species in the CMD pathway.

2.3. Computational Studies. To gain additional understanding of the role of pivalate in the CMD mechanism, the isolation

and characterization of a Pd(II) intermediate of general structure [(PCy₃)_nPd(Ar)(OPiv)] and its evaluation as a catalytically and kinetically competent species should be investigated. Unfortunately all attempts at synthesizing this potential catalytic intermediate were unsuccessful, leading us to examine its role through the use of computational studies.

2.3.1. Methods. DFT calculations were performed using the Gaussian 03 program.³⁷ Stationary points on the potential energy surface were obtained using the B3LYP exchange–correlation functional^{38,39} with the TZVP basis set⁴⁰ for all atoms except Pd. For Pd, the DZVP basis set⁴¹ was used. Tight SCF convergence criteria (10^{−8} a.u.) were used for all calculations. The converged wave functions were tested to confirm that they correspond to the ground-state surface. Harmonic frequency calculations were used to determine the nature of the stationary points. The analysis of two- and three-center bond orders were carried out using the AOMix program.⁴² Solvation energies of species in toluene were calculated using the gas-phase geometries and the PCM implicit solvent solvation model⁴³ with the UFF atomic radii. Gibbs free energies of different species in toluene were estimated by addition of the solvation energy Δ*G*_{solv} to gas-phase Gibbs free energies.

2.3.2. Pivalate As a Promoter of Phosphine Dissociation. KIE experiments and mechanistic data support a turnover-limiting C(sp³)–H bond cleavage *via* a base-enabled CMD transition state (*vide supra*). DFT calculations were performed to determine the ground state energies of various potential Pd(II) intermediates and CMD transition states (Figures 4–5).⁴⁴ Intermediates **III** and **IV**, resulting from PMe₃ dissociation from **II** and amide coordination through either the oxygen or nitrogen atom, are respectively 1.7 and 4.8 kcal/mol higher in energy than structure **II**. In intermediate **IV**, the nitrogen lone pair is no longer in conjugation with the amide carbonyl due to its coordination to Pd(II). κ²-Acetate complex **I** is 0.6 kcal/mol lower in energy than structure **II**. Therefore, prior to the rate-limiting CMD process (Figure 6), the thermodynamic equilibrium shifts toward intermediate **I**, a direct precursor to the inner-sphere pivalate (acetate for computational purposes)-enabled CMD TS.⁴⁵ The free energy of the CMD transition state **TS-I** is 29.1 kcal/mol and is slightly higher than the free energy of the corresponding transition state for intramolecular alkane arylation in the synthesis of dihydrobenzofurans (27.0 kcal/mol).^{3j} Similar to previous reports,^{3j,v} an agostic three-center two-electron interaction was found at the transition state between the Pd(II) center and the C–H σ bond being cleaved (Figure 6).

(37) Frisch, M. J. *Gaussian 03*, revision C.02; Gaussian, Inc.: Wallingford, CT, 2004.

(38) Becke, A. D. *J. Chem. Phys.* **1993**, *98*, 5648.

(39) Lee, C.; Yang, W.; Parr, R. G. *Phys. Rev. B* **1988**, *37*, 785.

(40) Schafer, A.; Huber, C.; Ahlrichs, R. *J. Chem. Phys.* **1994**, *100*, 5829.

(41) Godbout, N.; Salahub, D. R.; Andzelm, J.; Wimmer, E. *Can. J. Chem.* **1992**, *70*, 560.

(42) (a) Gorelsky, S. I.; Lever, A. B. P. *J. Organomet. Chem.* **2001**, *635*, 187. (b) Gorelsky, S. I. *AOMix: software for the MO Analysis*, revision 6.35; University of Ottawa: Ottawa, 2007.

(43) Barone, V.; Cossi, M.; Tomasi, J. J. *Comput. Chem.* **1998**, *19*, 404.

(44) PCy₃ was modeled as PMe₃ and pivalate as acetate to minimize computational costs.

(45) While this discussion does not take into consideration the generation of **II** (or **III**) from **I**, it is assumed that any transition states (or other intermediates) along these pathways are not energetically significant in the global reaction scheme since KIE studies reveal that C(sp³)–H bond cleavage is involved in the rate-determining step (Section 2.1).

(36) A 10-fold amount of carbonate and pivalate were used to mimic the relative base/palladium ratios that are found under the standard catalytic conditions. See Supporting Information for further experimental details.

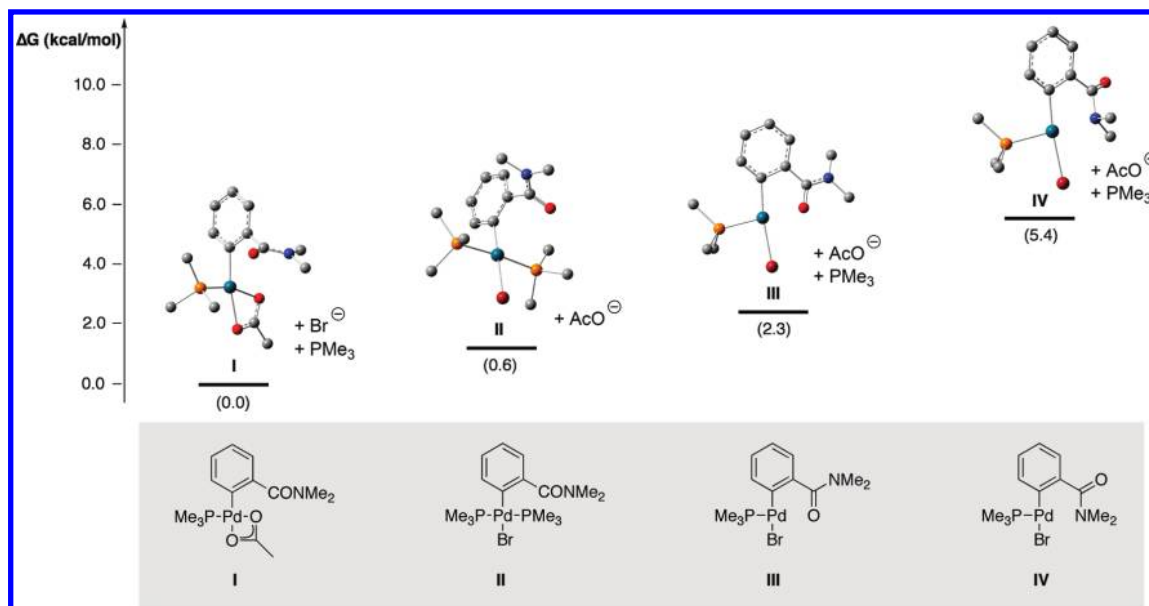


Figure 4. Gibbs free energies (at 298 K in toluene) of potential Pd(II) intermediates prior to the CMD transition state. Hydrogen atoms have been omitted for clarity.

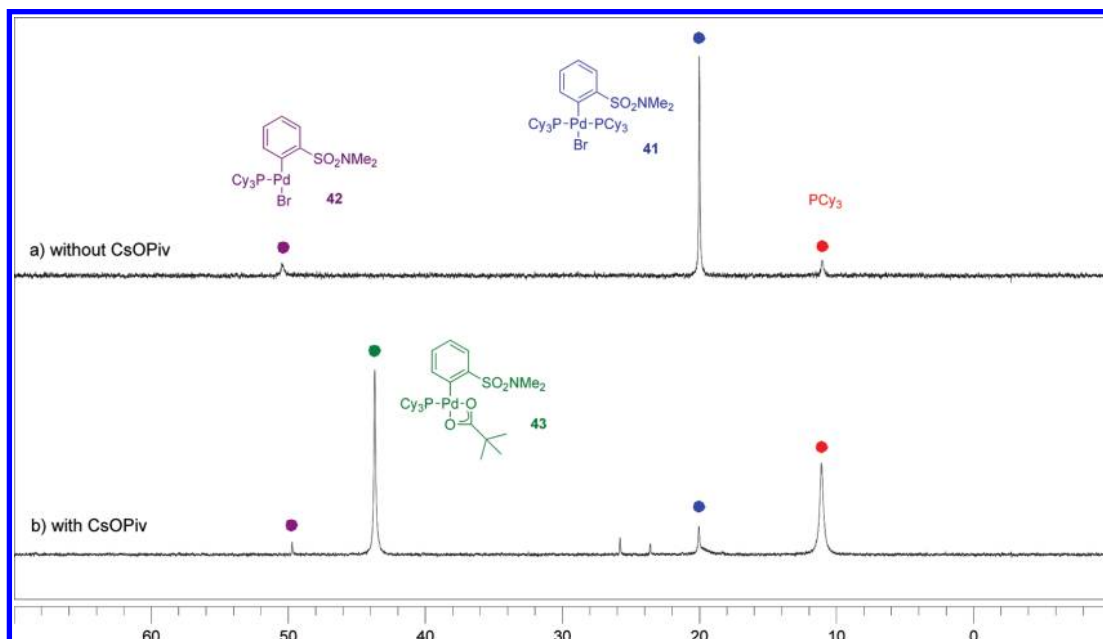


Figure 5. Observation of PCy₃ dissociation from Pd(II) intermediate **41** (a) in the absence of CsOPiv and (b) in the presence of 6 equiv of CsOPiv. Complex **41** and CsOPiv (if added) were stirred in mesitylene at 120 °C for 20 min after which time ³¹P NMR spectra were collected at 60 °C.

To lend additional support to the hypothesis that pivalate plays a crucial role in promoting phosphine dissociation from Pd(II) to increase the concentration of the reactive intermediate, stoichiometric reactions were performed with Pd(II) intermediate **41**. Side-by-side reactions of complex **41** and CsOPiv (if added) in mesitylene at 120 °C were carried out to observe the effect of added CsOPiv on the concentration of free PCy₃ in solution. The reaction outcome was monitored by ³¹P NMR (Figure 5). In the absence of CsOPiv, starting material **41** remains almost exclusively the sole product in solution (Figure 5a). Trace amounts of PCy₃ and proposed intermediate **42** could be detected. When the same experiment is performed in the presence of CsOPiv (6 equiv), very little starting complex **41** remains after 20 min at 120 °C. Instead, a significant amount of free PCy₃ can be detected with the simultaneous appearance

of a second signal at 43.7 ppm, which is proposed to correspond to κ^2 -pivalate complex **43** (Figure 5b). The relative concentrations of Pd(II) intermediates observed under these different reaction conditions support the results of DFT calculations in Figure 4 and provide additional evidence for the role of pivalate as a promoter of phosphine dissociation.

2.3.3. Role of Carbonate in Product Formation. Stoichiometric reactions revealed a lack of reactivity in the presence of only Cs₂CO₃ or CsOPiv as a source of base compared to a near quantitative product yield when both were added to the reaction mixture (Table 6, section 2.2.4). These results appear to indicate that both carbonate and pivalate play an active role in C–H bond cleavage. This apparent synergy has been investigated through the use of DFT calculations which reveal a highly reactant-biased potential energy surface for the C(sp³)–H bond

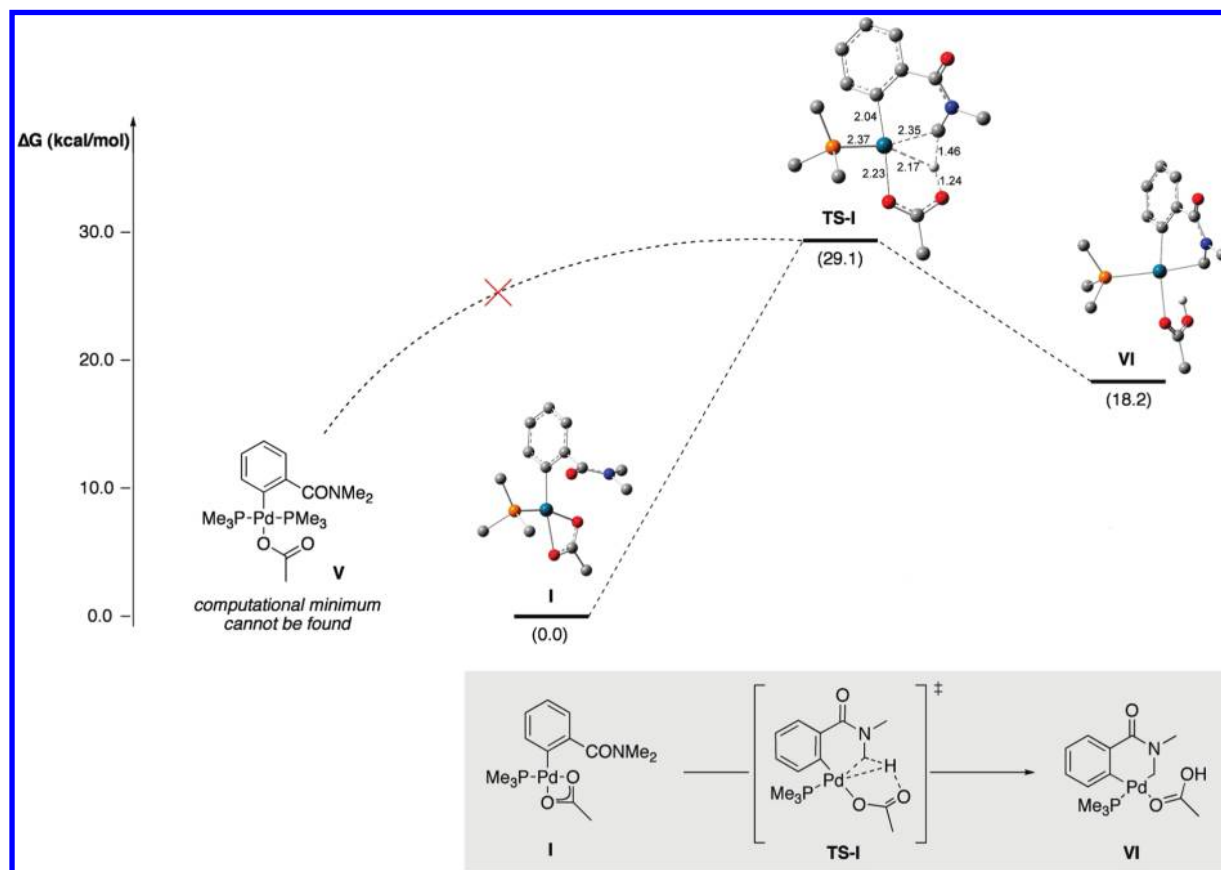
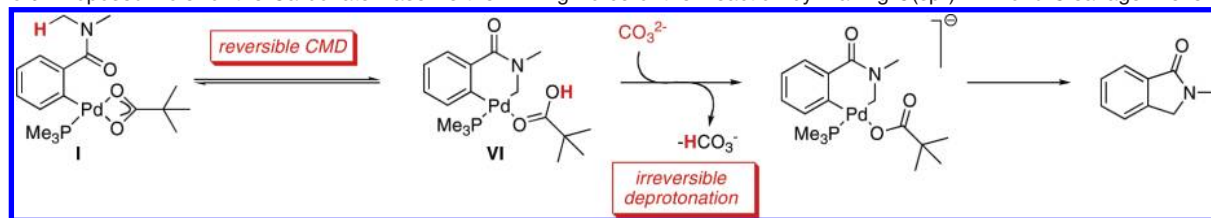


Figure 6. Gibbs free energies (at 298 K in toluene) of the formation of κ^1 -acetic acid complex **VI** from intermediate **I** via CMD transition state **TS-I** featuring an agostic Pd(II)...C–H interaction. Selected bond distances (Å) are indicated. Hydrogen atoms that do not participate in the CMD process have been omitted for clarity.

Scheme 9. Proposed Role for the Carbonate Base As the Driving Force of the Reaction by Making C(sp³)–H Bond Cleavage Irreversible



cleaving step (Figure 6). The κ^1 -pivalic (acetic) acid complex **VI**, resulting from pivalate (acetate)-enabled CMD transition state **TS-I**, is a highly energetic ground state structure ($\Delta G = 18.2$ kcal/mol relative to the reactant complex **I**). Unless H⁺ is quickly removed from the pivalic (acetic) acid ligand, **VI** can readily revert to the reactant complex **I**. Carbonate, or other bases, may be required as a driving force for the reaction, by sequestering H⁺ and pushing intermediate **VI** toward the desired product (Scheme 9). These conclusions are consistent with the experimental observation of low product yields in stoichiometric studies employing pivalate exclusively as the base (Table 6, entries 3 and 7).

Further computational studies revealed that pivalate (acetate) also plays a crucial role in blocking potential catalysis inhibition by excess phosphine in the reaction medium. A computational minimum for a bisphosphine κ^1 -acetate complex **V** was not found when the CMD transition state (**TS-I**) was collapsed back to starting material. Instead, the structure invariably reverts to κ^2 -acetate intermediate **I** (Figure 6). This suggests that **V** does not participate in the catalytic cycle.

These results, combined with previous experimental studies (see section 2.2.4), highlight the importance of *both* basic species in Pd(0)-catalyzed arylations at C(sp³)–H bonds. Not only does the pivalate act as the base which enables C–H bond cleavage, but it also increases the concentration of Pd(II) reactive intermediate **I** prior to the CMD reaction step while also preventing reaction inhibition by excess free phosphine in solution. The carbonate base in this system may also have a more active role in C(sp³)–H bond cleavage than previously believed by favoring product formation through the irreversible deprotonation of the post-CMD catalytic intermediate **VI**.

2.3.4. Effect of Nitrogen Basicity in C(sp³)–H Bond Cleavage. Catalyst sequestration studies (Scheme 4) and ³¹P NMR experiments (Scheme 3) suggest the formation of a problematic intermediate **2**, featuring nitrogen coordination to the Pd(II) center, as an explanation for the observed lack of reactivity with more Lewis basic nitrogen-containing substrates. While the generation of intermediate **2** effectively blocks product formation, it is interesting to investigate whether the change in electron density on the heteroatom affects other aspects of C–H

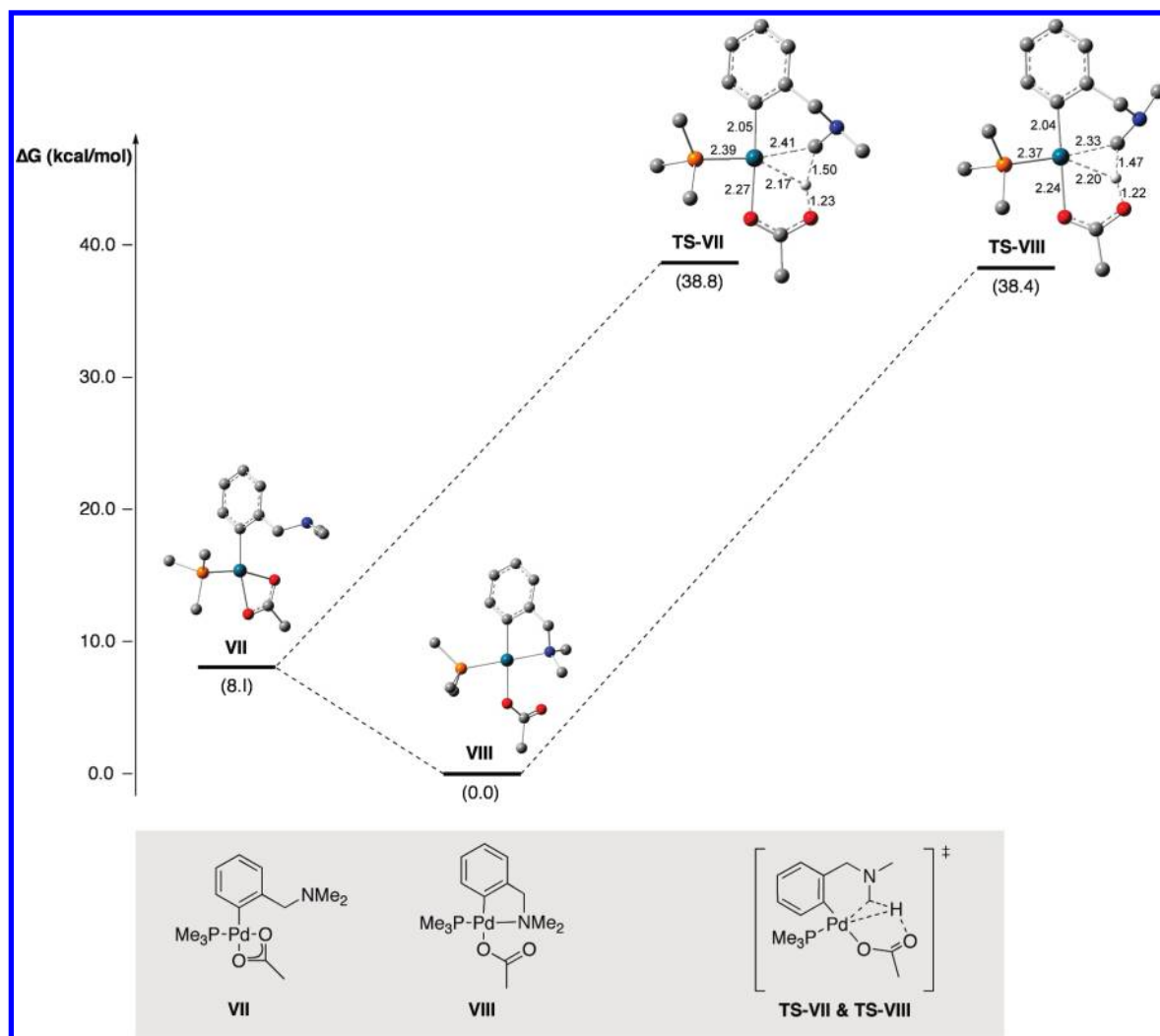


Figure 7. Gibbs free energies (at 298 K in toluene) of potential Pd(II) intermediates prior to the CMD transition state **TS-VIII** in the arylation of a C(sp³)-H bond adjacent to an amine. Selected bond distances (Å) in the CMD transition state are indicated. Hydrogen atoms that do not participate in the CMD process have been omitted for clarity.

bond cleavage to design future reaction substrates. To this effect, DFT calculations have been performed to investigate the alkane arylation of 2'-bromobenzyl-*N,N*-dimethylamine (Figure 7).

When the potential energy surfaces for C(sp³)-H bond cleavage in amine and amide substrates are compared, the explanation for the lack of reactivity with amine derivatives becomes apparent. In amide derivatives, κ^2 -acetate complex **I** is the direct precursor to CMD transition state **TS-I**, which is 29.1 kcal/mol uphill from this intermediate (Figure 6). However, in amine derivatives, κ^2 -acetate complex **VII** is not the most stable ground state structure; κ^1 -acetate complex **VIII** is 8.1 kcal/mol lower in energy and is the precursor to CMD transition state **TS-VIII**. This increase in the ground state stability of the intermediate prior to C-H bond cleavage leads to a significantly higher energy barrier for this transition state (38.4 kcal/mol). A second CMD transition state **TS-VII** for C(sp³)-H bond cleavage from κ^2 -acetate complex **VII** can also be found and is 38.8 kcal/mol higher in energy than the most stable ground state structure **VIII**. **TS-VII** and **TS-VIII** differ in the orientation of the lone pair and the substituents on the nitrogen atom (Figure 7).

These two possible CMD transition states (**TS-VII** and **TS-VIII**) exhibit features similar to those of **TS-I** (Figures 6 and 7). **TS-VII** and **TS-VIII** feature an agostic three-center two-

electron interaction between the Pd(II) atom and the C-H σ bond being cleaved. Similar bond lengths are observed for the atoms that participate in the concerted metalation-deprotonation process indicating that the degree of bond formation/bond cleavage in all three transition states is comparable and that increased nitrogen atom basicity does not affect the nature of the transition state for C(sp³)-H bond cleavage.

Combined with experimental observations (see section 2.1, Schemes 3–4), the results of this DFT study support the conclusion that the electron density on the nitrogen atom does not affect C(sp³)-H bond cleavage, or the properties of the C-H bond, but rather leads to more stable palladium-substrate interactions, rendering the energy barrier for C-H bond cleavage too high.

2.4. Kinetic Studies: Reagent Orders. Efforts in future catalyst and reaction design are best focused on accelerating the turnover limiting step of a catalytic cycle. To establish the reaction rate expression, kinetic studies were performed to determine the order in each component in the reaction of 2-bromo-*N,N*-dimethylbenzamide **12**.³² Initial rates were determined for reactions where the concentrations in starting material (Figure 8), palladium (Figure 9), ligand (Figure 10), and pivalate (Figure 11) were modified independently.

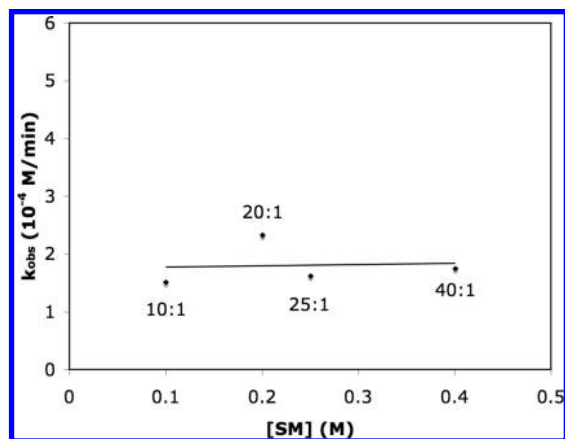


Figure 8. Dependence of the initial rate on the concentration of 2-bromo-*N,N*-dimethylbenzamide **12** (SM) (0.10–0.40 M). Conditions: $[\text{Pd}(\text{PCy}_3)_2] = 1.0 \times 10^{-2}$ M and $[\text{PivOH}] = 6.0 \times 10^{-2}$ M in 2.9 mL of mesitylene with 0.872 mmol of Cs_2CO_3 at 150 °C. Yields were determined by GC/MS using 1,3,5-trimethoxybenzene as an internal standard. Data labels represent **12**/palladium ratios.

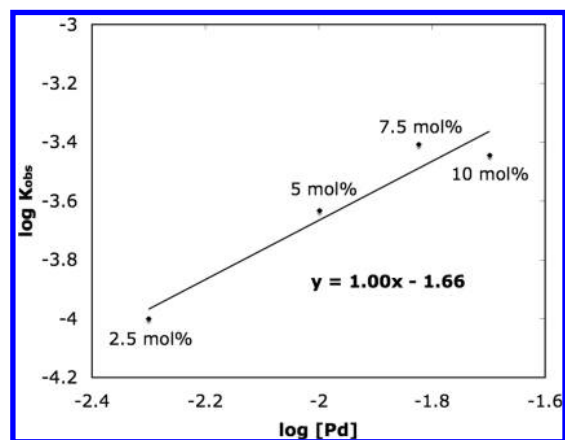


Figure 9. Dependence of the logarithm of the initial rate on the logarithm of the concentration of $\text{Pd}(\text{PCy}_3)_2$ (5.0×10^{-3} – 2.0×10^{-2} M). Conditions: [2-bromo-*N,N*-dimethylbenzamide **12**] = 0.20 M and $[\text{PivOH}] = 6.0 \times 10^{-2}$ M in 2.9 mL of mesitylene with 0.872 mmol of Cs_2CO_3 at 150 °C. Yields were determined by GC/MS using 1,3,5-trimethoxybenzene as an internal standard. Data labels represent the catalyst loading.

Plotting the initial rate against the concentration of 2-bromo-*N,N*-dimethylbenzamide **12** reveals that the reaction is zeroth-order in substrate (Figure 8), indicating that oxidative addition is not rate-determining. A plot of the logarithm of initial rates versus the logarithm of the concentration in palladium reveals a slope of 1.00 for catalyst loadings of 2.5, 5, 7.5, and 10 mol % (Figure 9). $\text{Pd}(\text{PCy}_3)_2$ was used as the palladium source instead of $\text{Pd}(\text{OAc})_2$ to avoid any potential rate effects due to the presence of additional acetate ions in solution. The slope of 1.00 is indicative of a first-order rate dependence in catalyst loading. Next, the effect of excess phosphine on the rate was examined. The plot of initial rates versus the concentration of phosphine uncovers that PCy_3/Pd ratios in excess of 2:1, i.e. the standard catalytic conditions, do not inhibit catalysis (Figure 10). This correlates with computational results suggesting that pivalate coordination to $\text{Pd}(\text{II})$ may prevent inhibition of the CMD step through phosphine coordination to $\text{Pd}(\text{II})$ (see section 2.3.3).

Finally, the effect of pivalate concentrations on initial rates was also examined. A linear increase in initial rate is observed for 0.5:1, 1:1, 2:1, and 3:1 pivalate/palladium ratios (Figure 11).

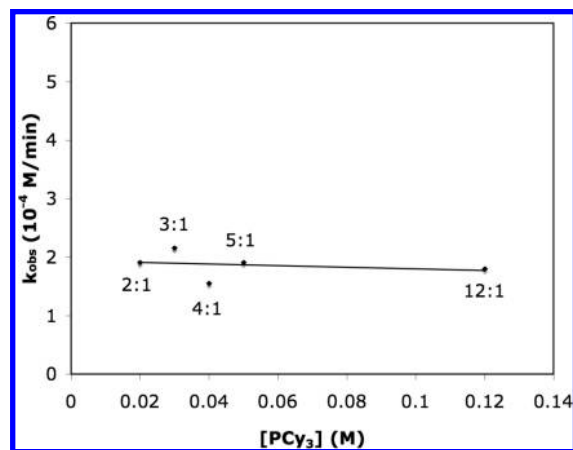


Figure 10. Dependence of the initial rate on the concentration of $\text{PCy}_3 \cdot \text{HBF}_4$ (2.0×10^{-2} – 1.2×10^{-1} M). Conditions: [2-bromo-*N,N*-dimethylbenzamide **12**] = 0.20 M, $[\text{Pd}(\text{OAc})_2] = 1.0 \times 10^{-2}$ M, and $[\text{PivOH}] = 6.0 \times 10^{-2}$ M in 2.9 mL of mesitylene with 0.872–1.16 mmol of Cs_2CO_3 at 150 °C. Yields were determined by GC/MS using 1,3,5-trimethoxybenzene as an internal standard. Data labels represent phosphine/palladium ratios.

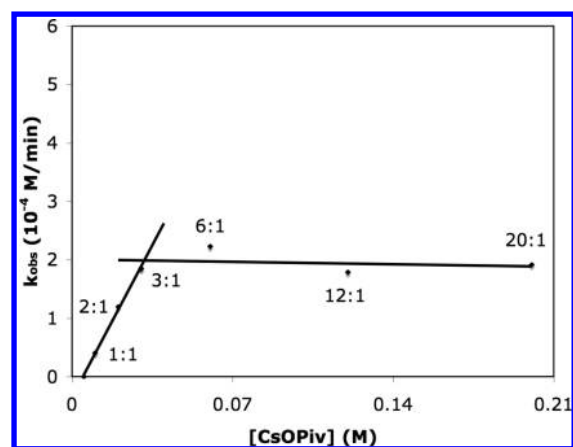


Figure 11. Dependence of the initial rate on the concentration of CsOPiv (5.0×10^{-3} – 2.0×10^{-1} M). Conditions: [2-bromo-*N,N*-dimethylbenzamide **12**] = 0.20 M and $[\text{Pd}(\text{PCy}_3)_2] = 1.0 \times 10^{-2}$ M in 2.9 mL of mesitylene with 0.872 mmol of Cs_2CO_3 at 150 °C. Yields were determined by GC/MS using 1,3,5-trimethoxybenzene as an internal standard. Data labels represent pivalate/palladium ratios.

The dependence of the initial rate on the concentration of pivalate changes from first- to zeroth-order, revealing saturation kinetics when pivalate/palladium ratios exceed 3:1. Figure 11 also reveals an optimal rate acceleration at ~30 mol % pivalate additive (6:1 pivalate/palladium), further validating the selection of this amount of pivalic acid additive during reaction development (section 2.1).

From this kinetic data, the rate expression for the formation of isoindolinones by alkane arylation under standard catalytic conditions can be expressed as

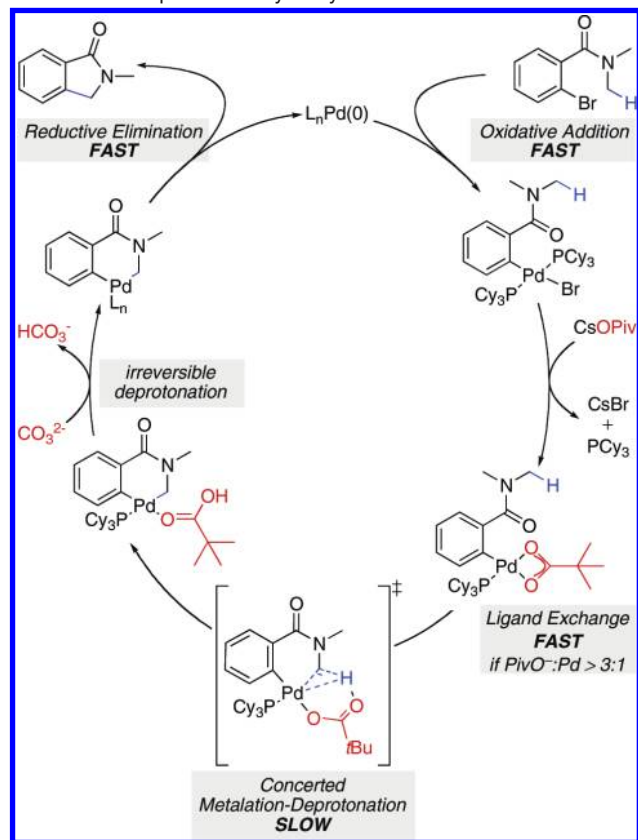
$$\text{rate} = k[\text{Pd}][\text{PivO}^-]^n$$

$$n = 1 \text{ when } \text{PivO}^-/\text{Pd} < 3:1$$

$$n = 0 \text{ when } \text{PivO}^-/\text{Pd} > 3:1$$

2.5. Proposed Catalytic Cycle. Based on these mechanistic, kinetic, and computational results, a clearer picture of the catalytic cycle for arylation at $\text{C}(\text{sp}^3)\text{--H}$ bonds emerges (Scheme 10). Oxidative addition of the desired aryl halide starting material to $\text{Pd}(0)$ occurs rapidly under the reaction

Scheme 10. Proposed Catalytic Cycle



conditions to afford a Pd(II) intermediate. This species may undergo a rapid ligand exchange, replacing the halide by a pivalate ion generated *in situ* from the reaction of pivalic acid with carbonate. Kinetic studies reveal the importance of pivalate concentration on this elementary reaction step as PivO[−]/Pd ratios greater than 3:1 lead to palladium saturation in this ligand. Computational and experimental results further support the formation of a κ^2 -pivalate Pd(II) intermediate as the direct precursor to the CMD reaction step, which is enabled by the pivalate ligand. The post-CMD intermediate is deprotonated by the carbonate base which acts as the driving force of the reaction by making C(sp³)-H bond cleavage irreversible. The cycle is completed by rapid reductive elimination of the desired product with regeneration of the Pd(0) catalyst.

3. Conclusion

In conclusion, the Pd(0)-catalyzed intramolecular arylation at C(sp³)-H bonds adjacent to amides and sulfonamides has been developed. Tuning the Lewis basicity of the nitrogen atom is crucial for the transformation. Mechanistic studies confirmed that C(sp³)-H bond cleavage is the rate-limiting step of the catalytic cycle. The isolation of a Pd(II) intermediate has allowed, for the first time, a direct evaluation of the C-H bond cleaving step in Pd(0)-catalyzed C-C bond formation at nonacidic C(sp³)-H bonds. This catalytic event appears to occur through a CMD pathway featuring cooperative assistance by both pivalate and carbonate bases. Computational studies further elucidated a second crucial role for the pivalate additive as a promoter of phosphine dissociation prior to the CMD transition state. These mechanistic findings highlight the importance of

basic additives in catalytic transformations at C-H bonds. The notion of multiple roles for a single additive at the metal center should influence future reaction development in this field.

4. Experimental Section

Representative Procedure for the Alkane Arylation of N-Methylamides. A Radley test tube equipped with a magnetic stir bar and a rubber septum was flame-dried under vacuum and a constant flow of argon. Once the test tube was cooled to room temperature, the vacuum was removed. Subsequent manipulations were performed under constant argon flow unless noted otherwise to give reproducible results. The flame-dried test tube was brought into the glovebox, and dry Rb₂CO₃ (201 mg, 0.872 mmol, 1.5 equiv) was added after which it was brought back onto the benchtop. Pd(OAc)₂ (6.5 mg, 0.029 mmol, 5 mol %) and PCy₃·HBF₄ (21.4 mg, 0.0581 mmol, 10 mol %) were quickly added, and the test tube was put under vacuum for 10 min and refilled with argon (×3). 2-Bromo-N-cyclohexyl-N-methylbenzamide (**8**) (172.1 mg, 0.5811 mmol, 1.0 equiv) and PivOH (17.8 mg, 0.174 mmol, 30 mol %) were added as degassed stock solutions in mesitylene (0.32 and 0.16 M respectively) after which the tube was sealed with parafilm and electrical tape around the rubber septum and placed in a preheated oil bath at 150 °C for 16 h. Upon cooling to room temperature, the reaction was quenched with EtOAc (1 mL) and transferred to a 200 mL round-bottom flask containing 60 mL of CH₂Cl₂ and 60 mL of a saturated solution of NH₄Cl. After stirring at room temperature for 15–30 min, the mixture was separated and the aqueous layer was extracted with 60 mL of CH₂Cl₂ (×2). The combined organic phases were washed with brine, dried with Na₂SO₄, concentrated under reduced pressure, and purified by silica gel flash chromatography (30% EtOAc in petroleum ether) to afford **9** as a beige solid in 83% yield. ¹H NMR (400 MHz, CDCl₃, 293 K, TMS) δ 7.86–7.84 (m, 1H), 7.54–7.52 (m, 1H), 7.47–7.44 (m, 2H), 4.35 (s, 2H), 4.30–4.22 (m, 1H), 1.89–1.45 (m, 10H). ¹³C NMR (100 MHz, CDCl₃, 293 K, TMS) δ 168.0, 141.4, 133.6, 131.1, 128.0, 123.7, 122.8, 50.6, 46.1, 31.6, 25.8, 25.7. HRMS Calculated for C₁₄H₁₇NO (M⁺) 215.1310, Found 215.1288. IR (ν_{max}/cm^{−1}) 2931, 2852, 1681, 735 cm^{−1}. R_f 0.27 (30% EtOAc in petroleum ether). Melting Point 78–82 °C.

Acknowledgment. We thank NSERC and the University of Ottawa for support of this work. The Research Corporation, Boehringer Ingelheim (Laval), Merck Frosst Canada, Merck Inc., Eli Lilly, Amgen, and Astra Zeneca Montreal are thanked for additional unrestricted financial support. S.R. thanks NSERC for a postgraduate scholarship (CGS-D), and B.C. thanks NSERC for an undergraduate summer research award. Prof. Muralee Murugesu and Dr. Tara Burchell are gratefully acknowledged for assistance in obtaining and solving the crystal structure. Prof. Tom K. Woo is thanked for CFI- and ORF-funded computing facilities. Prof. Louis Barriault, Prof. André Beauchemin, and Dr. Louis-Charles Campeau are thanked for critical reading of this manuscript. Dr. Benoît Liégault is also thanked for assistance in the preparation of certain figures and critical evaluation of this manuscript. Prof. Keith Fagnou passed away on November 11, 2009.

Supporting Information Available: Detailed experimental procedures for the synthesis of all compounds. Characterization data and ¹H and ¹³C NMR spectra for all new compounds. Kinetic data, computational details and crystallographic information files. Complete ref 37. This material is available free of charge via the Internet at <http://pubs.acs.org>.

JA103081N